CONFIDENTIAL



Copy No. 314

RM No. A8I16

NACA RM No. A8I16



# RESEARCH MEMORANDUM

## AERODYNAMIC CHARACTERISTICS AT SUBSONIC AND SUPERSONIC MACH NUMBERS OF A THIN TRIANGULAR WING OF ASPECT RATIO 2. I - MAXIMUM THICKNESS AT 20 PERCENT OF THE CHORD

By Robert E. Berggren and James L. Summers

Ames Aeronautical Laboratory
Moffett Field, Calif.



WASHINGTON
November 19, 1948

CONFIDENTIAL

NATIONAL ADVISORY COMMITTEE FOR AERONAUTICS

RESEARCH MEMORANDUM

# AERODYNAMIC CHARACTERISTICS AT SUBSONIC AND SUPERSONIC MACH NUMBERS OF A THIN TRIANGULAR WING OF ASPECT RATIO 2.

## I – MAXIMUM THICKNESS AT 20 PERCENT OF THE CHORD

By Robert E. Berggren and James L. Summers

## SUMMARY

This report presents the results of a wind-tunnel investigation conducted to determine the effects of Mach number on the aerodynamic characteristics of a wing of triangular plan form. The wing was of aspect ratio 2 and of symmetrical double-wedge section with 5-percent chord maximum thickness at 20 percent of the chord. The tests were conducted at Mach numbers from 0.50 to 0.975 and 1.09 to 1.49 and at Reynolds numbers ranging from 0.67 to 0.85 million.

The experimental results indicate chiefly that (a) the lift-curve slope increased steadily with an increase in subsonic Mach number and decreased gradually with Mach number above 1.12; (b) the aerodynamic center shifts from 40 to 50 percent of the mean aerodynamic chord in the subsonic Mach number range and remains at approximately 51 percent of the mean aerodynamic chord throughout the supersonic Mach number range; (c) the minimum drag coefficient is essentially constant at subsonic Mach numbers and at supersonic Mach numbers above 1.2, but increases appreciably with Mach number in the portion of the supersonic range below 1.2; (d) the drag due to lift decreases continuously in the subsonic range up to a Mach number of 0.94, but, in the supersonic Mach number range, the variation is reversed and a continuous increase occurs with increasing Mach number; and (e) calculated characteristics except for minimum drag coefficient were in reasonable agreement with the experimental characteristics.

## INTRODUCTION

The use of highly swept or low-aspect-ratio wings has frequently been proposed for aircraft designed to operate at supersonic Mach

numbers. Theoretical studies by Jones (references 1 and 2) and Puckett and Stewart (reference 3) have indicated that the low-aspect-ratio triangular wing with apex forward is a promising plan form for this application. The present investigation was undertaken in the Ames 1- by 3-1/2-foot high-speed wind tunnel to determine experimentally the principal aerodynamic characteristics of a low-aspect-ratio triangular wing at subsonic and supersonic Mach numbers and to compare these characteristics with those from theoretical calculations.

The wing was selected on the basis of certain theoretical predictions of Puckett and Stewart to provide minimum pressure drag at moderately supersonic Mach numbers for a triangular wing of practical thickness. The wing was of aspect ratio 2 and had a symmetrical double-wedge section. The maximum thickness was 5 percent and was located at 20 percent of the chord.

## SYMBOLS

| | |
|---|---|
| $b$ | span of wing, feet |
| $c$ | local wing chord, feet |
| $\bar{c}$ | mean aerodynamic chord $\left(\frac{\int_0^{b/2} c^2\,dy}{\int_0^{b/2} c\,dy}\right)$, feet |
| $C_D$ | drag coefficient $\left(\frac{\text{drag}}{qS}\right)$ |
| $C_{D_{min}}$ | minimum drag coefficient |
| $\Delta C_D$ | change in drag coefficient from value of minimum drag coefficient $(C_D - C_{D_{min}})$ |
| $\frac{\Delta C_D}{\Delta C_L{}^2}$ | drag-rise factor |
| $C_L$ | lift coefficient $\left(\frac{\text{lift}}{qS}\right)$ |
| $\Delta C_L$ | change in lift coefficient from the value at minimum drag coefficient $(C_L - C_{L_{D=min}})$ |
| $\frac{dC_L}{d\alpha}$ | lift-curve slope at zero lift coefficient, per degree |
| $C_m$ | pitching-moment coefficient $\left(\frac{\text{moment about centroid of area of wing}}{qS\bar{c}}\right)$ |

| | |
|---|---|
| $\frac{L}{D}$ | lift–drag ratio $\left(\frac{\text{lift}}{\text{drag}}\right)$ |
| $\left(\frac{L}{D}\right)_{max}$ | maximum lift–drag ratio |
| M | free–stream Mach number |
| q | free–stream dynamic pressure $(\frac{1}{2}\rho V^2)$, pounds per square foot |
| R | free–stream Reynolds number referred to the mean aerodynamic chord |
| S | wing area, square feet |
| V | free–stream velocity, feet per second |
| y | spanwise distance from the wing root–chord line, feet |
| $\alpha$ | angle of attack, degrees |
| $\rho$ | free–stream mass density, slugs per cubic foot |

## APPARATUS AND TESTS

The tests were performed in the Ames 1– by 3–1/2–foot high–speed wind tunnel, which is a closed–throat tunnel, fitted with a flexible throat to provide variations of supersonic speeds up to a Mach number of 1.5. A diagrammatic sketch of the throat section is given in figure 1. The model (fig. 2) was constructed of steel according to the dimensions of figure 3. Leading and trailing edges of the wing were maintained sharp (less than 0.002–in. radii) throughout the tests. The wing surfaces were ground but not polished.

The wing was mounted in a horizontal plane in a slender body of revolution (fig. 2) having the minimum size consistent with its function as an adequate support. A series of identical bodies (fig. 3), sting supported at different angles of attack, was employed interchangeably to vary the wing angle of attack.

A three–component electrical strain–gage balance was used to measure the lift, drag, and pitching moment of the model. Measurements of the pressure acting on the base of the body were made simultaneously with the force measurements.

Measurements of lift, drag, and pitching moment were taken at intervals in the Mach number ranges of 0.50 to 0.975 and 1.09 to 1.49 and at angles of attack from approximately $-3^\circ$ to $9^\circ$. Reynolds number, based on the mean aerodynamic chord, varied from $0.67 \times 10^6$ at 0.50 Mach number to $0.83 \times 10^6$ at 1.49 Mach number. Wind-tunnel-choking considerations precluded testing at Mach numbers between 0.975 and 1.09.

## REDUCTION OF DATA

Lift, drag, and pitching-moment coefficients are based on the wing area including that portion which was enclosed within the body. Pitching-moment coefficients are referred to the centroid of wing area and are based on the mean aerodynamic chord.

Corrections for wind-tunnel-wall interference were made at subsonic Mach numbers to both the measured angles of attack and drag coefficients by the method of reference 4. These corrections, demonstrated in reference 5 to be independent of Mach number, were:

$$\Delta\alpha = 0.424\ C_L$$

$$\Delta C_D = 0.0075\ C_L^2$$

The drag forces were also corrected for the effects of the buoyant pressure gradients existing in the wind tunnel. This correction was less than 2 percent of the minimum drag at all Mach numbers. No corrections were made for any possible inclination of the air stream. The tunnel blockage corrections were determined to be negligible and were not applied to the test data.

The drag data were corrected for the interference arising from the close proximity of the balance cap to the afterend of the body. This interference is assumed to be confined to the base of the body at all Mach numbers. Theoretical computations have indicated this assumption to be essentially correct at subsonic Mach numbers. On the basis of a discussion contained in reference 6 this assumption is also believed to be valid at the supersonic Mach numbers. The effect of this interference is to change the pressure at the base of the body from that which would exist in the absence of the balance cap. To compensate for the effect of this interference, which is believed to vary with Mach number, the measured base pressure has been adjusted to correspond to the static pressure of the free stream. Thus, the adjusted drag is the measured drag of the wing and body minus the base drag of the body.

## RESULTS AND DISCUSSION

The results of the tests are presented in figure 4 as plots of lift coefficient as a function of angle of attack, and pitching-moment coefficient, drag coefficient, and lift-drag ratio as functions of lift coefficient for each test Mach number. Figures 5 through 11 are derived from figure 4 and show the variation with Mach number of certain of the aerodynamic parameters. Representative schlieren photographs of the model at various Mach numbers are presented in figure 12, part (a) being included to show the optical defects of the tunnel windows.

For purposes of correlation, characteristics obtained from references 7 and 8 at Reynolds numbers of $15.4 \times 10^6$ and $1.8 \times 10^6$, respectively, and reference 9 for a Mach number range of 0.50 to 0.95 and a Reynolds number of $5.3 \times 10^6$ on wings of similar plan form and section are compared with the results of the present test. Further comparison with the results of the present investigation is provided by including data from reference 6 for the identical configuration and a closely comparable Reynolds number.

The forces and moments of the wing alone from the present test could not be readily separated from those of the wing-body combination because of the difficulty in determining the wing-body interference. The coefficients presented, therefore, represent the results of the combination and not of the wing alone. The contribution of the body to the lift and pitching moment is believed to be small. However, the drag produced by the body is of appreciable magnitude and this fact should be borne in mind in a study of the drag characteristics. A description of the influence of the body upon the characteristics of the combination is given in reference 6.

### Lift Characteristics

The theoretical lift curves shown in figure 4 are for the wing alone and were determined by the methods of references 10 and 3 for the subsonic and supersonic Mach numbers, respectively.

The increase in the experimental lift-curve slope with angle of attack, apparent in the subsonic data (fig. 4) up to angles of attack of about $7^\circ$, is typical of wings of very low aspect ratio. Results from tests at a higher Reynolds number (reference 7) show lift curves of a similar nature. The displacements of the lift curves from zero angle of attack at zero lift coefficient to be noted at

several Mach numbers were caused by stream inclination for which corrections were not made.

The respective variations with Mach number of lift coefficient at constant angles of attack and of lift-curve slope are shown in figures 5 and 6. From these figures it can be seen that there are no abrupt changes in these two parameters with Mach number. The experimental values of the lift-curve slope (fig. 6) increase with Mach number in the subsonic range and decrease with Mach number in the supersonic range above a Mach number of 1.12. The discrepancy in the magnitudes of the theoretical and experimental lift-curve slopes is evidently due to the influence of the body and to second-order effects of thickness of the airfoil which are not considered in either the subsonic or supersonic theories. The agreement with the present investigation of the lift-curve slopes of references 6, 7, 8, and 9 is reasonable if consideration is given to the differences in Reynolds number.

It appears that there are no abrupt changes near the Mach number of unity in either the lift coefficient at constant angles of attack (fig. 5) or lift-curve slope (fig. 6). Data obtained from tests by the NACA wing-flow method (reference 11) on a similar wing at a Reynolds number of approximately $1.0 \times 10^6$ have revealed no erratic changes within the range of Mach numbers from 0.975 to 1.09 which were not covered in the present investigation.

## Pitching-Moment Characteristics

It can be seen that the variation in pitching-moment coefficient with lift coefficient, shown in figure 4 for various Mach numbers, is continuous and almost linear. The aerodynamic center location, plotted against Mach number in figure 7, was determined from the slope of the pitching-moment curve (fig. 4) at zero lift coefficient. Figure 7 indicates that the travel of the aerodynamic center with Mach number is 10 percent of the mean aerodynamic chord in the subsonic range. At the supersonic Mach numbers the position of the aerodynamic center remains within 2 percent of that predicted by the linear theory (50 percent of the mean aerodynamic chord). The results of this investigation are in good agreement with reference 9 at the lower subsonic Mach numbers (below 0.8) but differ considerably at the high subsonic Mach numbers. The agreement of reference 6 with the results of the present test is excellent.

## Drag Characteristics

The calculated drag polars in figure 4 for the supersonic Mach number range are for the wing alone and were obtained by summing the

pressure drag and skin-friction drag computed by the methods of references 3 and 12, respectively. Because the distribution of laminar and turbulent flow over the wing was unknown, boundaries representing pressure drag plus complete laminar skin friction and pressure drag plus complete turbulent skin friction have been indicated. Values of skin-friction coefficients corresponding to incompressible flow were assumed in the calculations. The experiments of references 12 and 13 would appear to justify this assumption. The experimental drag polars presented in figure 4 for the Mach numbers of 1.09 and 1.12 are seen to exhibit a lower rate of change of drag coefficient with lift coefficient than those for other supersonic Mach numbers, or those calculated for these two Mach numbers. Possible reasons for this low rate of drag rise are discussed later in the discussion of the drag-rise factor.

The variation of drag coefficient with Mach number at constant values of lift coefficient is shown in figure 8. As would be expected from examination of the polars of figure 4, quite low values of drag coefficient at the higher lift coefficients are evident at the lower supersonic Mach numbers.

The character of these curves may be more readily analyzed by considering the change in drag coefficient accompanying a change in lift coefficient, that is, the drag due to lift. This quantity may be conveniently represented, because of the parabolic nature of the experimental polars, by a dimensionless parameter termed the "drag-rise factor" which is defined as $\Delta C_D/\Delta C_L^2$.

The drag-rise factor, plotted in figure 9 for the configuration of this investigation, exhibits the same character of variation with Mach number as the drag coefficient at constant lift coefficient (fig. 8). If the wing under investigation be considered as a flat-plate airfoil, realizing no leading-edge suction, the drag-rise factor can be equated to the reciprocal of the lift-curve slope. The reciprocal of the lift-curve slope has also been plotted in figure 9. In this figure the effect of Mach number on these two quantities is indicated to be essentially identical except in the region between Mach numbers 0.9 and 1.2.

The low values of the drag-rise factor at Mach numbers from 1.09 to approximately 1.17 appear questionable. No suitable explanation has been found for these apparently low values; however, for the following reasons they are believed to be the result of a wind-tunnel interference rather than genuine aerodynamic effects:

1. The air stream is known to contain random shock waves at the low supersonic Mach numbers, examples of which are indicated by arrows in figures 12(d) and (e).

2. Reflections from the tunnel walls of the shock waves originating at the body nose and point of juncture of wing and body impinged upon the model at Mach numbers from 1.09 to 1.17 and may have produced a buoyant pressure field in a direction to decrease the drag. (The reflected waves cannot be seen in fig. 12 because the optical axis of the schlieren system is parallel, not perpendicular, to the 1-foot dimension of the wind tunnel.)

3. At Mach number 1.09, a strong normal shock wave was located adjacent to the trailing edge of the wing. (See figs. 12(c) and (d).) The higher pressure after the shock wave may have been transmitted as a pressure disturbance through the subsonic wake of the model to reduce the drag below that which would occur in the absence of this wave.

The variation of minimum drag coefficient with Mach number is shown in figure 10. It will be noted from an examination of this figure that the drag divergence at high subsonic Mach numbers usually associated with unswept wings of higher aspect ratio does not occur for this configuration. In fact, the variation of minimum drag coefficient with Mach number in the entire subsonic range is quite small. Compared to the results of references 7 and 8, with consideration given to the friction drag of the body and to the influence of Reynolds number, the values of this coefficient appear satisfactory.

A comparison with the results of reference 9 shows a lack of agreement in both the magnitude and the rate of rise with Mach number of the minimum drag coefficient. It should be noted that the results of reference 9 were obtained for a semispan model mounted on a turntable in the floor of the tunnel. This reference indicates that, because of leakage of air through the gap between the turntable and the tunnel floor, the variation with Mach number of the minimum drag coefficient is subject to question. Also, the magnitude of the minimum drag coefficient of reference 9 may be somewhat in error because of the large drag-tare correction necessary (approximately 50 percent of the minimum drag coefficient).

In the range of Mach numbers above approximately 1.2, the variation of minimum drag coefficient with Mach number compares favorably with the predicted variation. The absolute values, however, are greater than those indicated by the theoretical upper limit.

This result may be attributed to the friction drag of the body and to possible boundary-layer-separation effects, neither of which was considered in the theoretical calculations.

The agreement of the results of the present investigation at the highest supersonic Mach number with that of reference 6 is considered satisfactory.

Maximum lift-drag ratio as affected by Mach number is shown in figure 11. It is observed that, at subsonic Mach numbers, the maximum lift-drag ratio remained fairly constant. At supersonic Mach numbers, increases in both minimum drag and drag due to lift caused this ratio to decrease. The high maximum lift-drag ratios at the lower supersonic Mach numbers can probably be attributed to the unexpectedly low drag values observed in this range.

At subsonic Mach numbers, the difference between the results of the subject investigation and those of references 7, 8, and 9 may again possibly be attributed to differences in Reynolds number and to the influence of the body present in this investigation. The agreement with the results of reference 6 is good. The experimental values are somewhat lower than the calculated values since the latter include neither the effect of the friction drag of the body nor the change in skin-friction drag with angle of attack.

## CONCLUSIONS

The results of wind-tunnel tests of a thin triangular wing of aspect ratio 2 and a double-wedge profile through the Mach number ranges of 0.50 to 0.975 and 1.09 to 1.49 indicate the following:

1. The lift-curve slope increased steadily with an increase in subsonic Mach number and decreased gradually with Mach number above 1.12.

2. The aerodynamic center shifted from 40 to 50 percent of the mean aerodynamic chord with Mach number at subsonic Mach numbers. At supersonic Mach numbers the aerodynamic center remained near the centroid of area.

3. The minimum drag coefficient remained essentially constant at subsonic Mach numbers and at supersonic Mach numbers above 1.2, but increased appreciably with Mach number in the portion of the supersonic range below 1.2.

4. A decrease in drag due to lift resulted from an increase in subsonic Mach number and a subsequent rise in drag due to lift resulted from an increase in Mach number above 1.09.

5. Theoretical calculations, except for minimum drag coefficient, were in reasonable agreement with the experimental characteristics.

Ames Aeronautical Laboratory,
National Advisory Committee for Aeronautics,
Moffett Field, Calif.

## REFERENCES

1. Jones, Robert T.: Properties of Low-Aspect-Ratio Pointed Wings at Speeds Below and Above the Speed of Sound. NACA TN No. 1032, 1946.

2. Jones, Robert T.: Estimated Lift-Drag Ratios at Supersonic Speed. NACA TN No. 1350, 1947.

3. Puckett, A. E., and Stewart, H. J.: Aerodynamic Performance of Delta Wings at Supersonic Speeds. Jour. Aero. Sci., vol. 14, no. 10, Oct. 1947, pp. 567-578.

4. Glauert, H.: Wind-Tunnel Interference of Wings, Bodies, and Airscrews. British R & M No. 1566, Sept. 1933.

5. Goldstein, S., and Young, A. D.: The Linear Perturbation Theory of Compressible Flow With Applications to Wind-Tunnel Interference. British R & M No. 1909, July 1943.

6. Vincenti, Walter G., Nielsen, Jack N., and Matteson, Frederick H.: Investigation of Wing Characteristics at a Mach Number of 1.53. I - Triangular Wings of Aspect Ratio 2. NACA RM No. A7I10, 1947.

7. Anderson, Adrien E.: An Investigation at Low Speed of a Large-Scale Triangular Wing of Aspect Ratio Two. I - Characteristics of a Wing Having a Double-Wedge Airfoil Section With Maximum Thickness at 20-Percent Chord. NACA RM No. A7F06, 1947.

8. Rose, Leonard M.: Low-Speed Investigation of a Small Triangular Wing of Aspect Ratio 2.0. I - The Effect of Combination With a Body of Revolution and Height Above a Ground Plane. NACA RM No. A7K03, 1948.

9. Edwards, George G., and Stephenson, Jack D.: Tests of a Triangular Wing of Aspect Ratio 2 in the Ames 12-Foot Pressure Wind Tunnel. I - The Effect of Reynolds Number and Mach Number on the Aerodynamic Characteristics of the Wing With Flaps Undeflected. NACA RM No. A7K05, 1948.

10. DeYoung, John: Theoretical Additional Span Loading Characteristics of Wings With Arbitrary Sweep, Aspect Ratio, and Taper Ratio. NACA TN No. 1491, 1947.

11. Rathert, George A., and Cooper, George E.: Wing-Flow Tests of a Triangular Wing of Aspect Ratio 2. I - Effectiveness of Several Types of Trailing-Edge Flaps on Flat-Plate Models. NACA RM No. A7G18, 1947.

12. Theodorsen, Theodore, and Regier, Arthur: Experiments on Drag of Revolving Discs, Cylinders, and Streamline Rods at High Speeds. NACA TR No. 793, 1944.

13. Keenan, Joseph H., and Neumann, Ernest P.: Friction in Pipes at Supersonic and Subsonic Velocities. NACA TN No. 963, 1945.

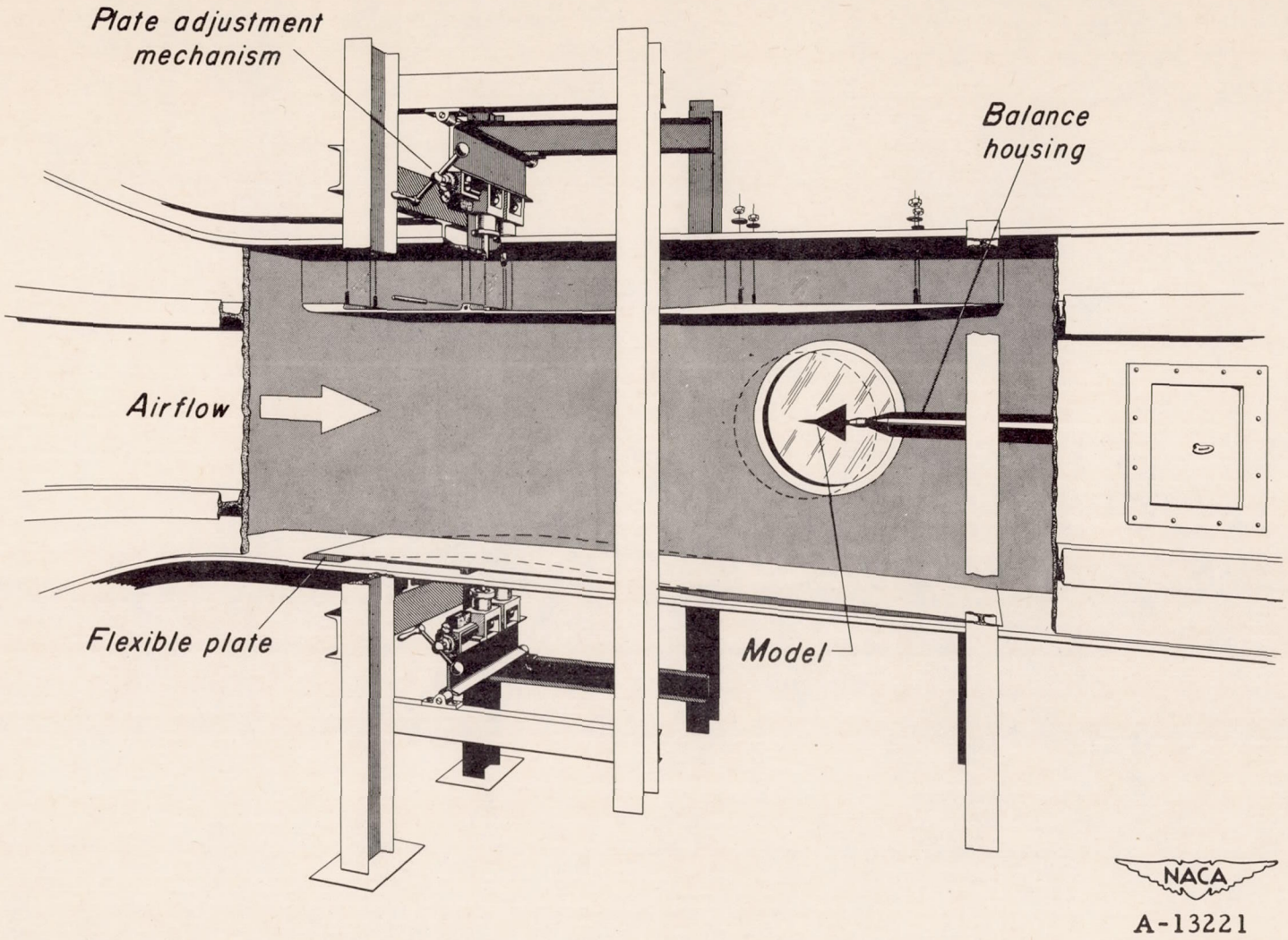


Figure 1.- Illustration of the flexible-throat mechanism in the Ames 1- by 3-1/2-foot high-speed wind tunnel.

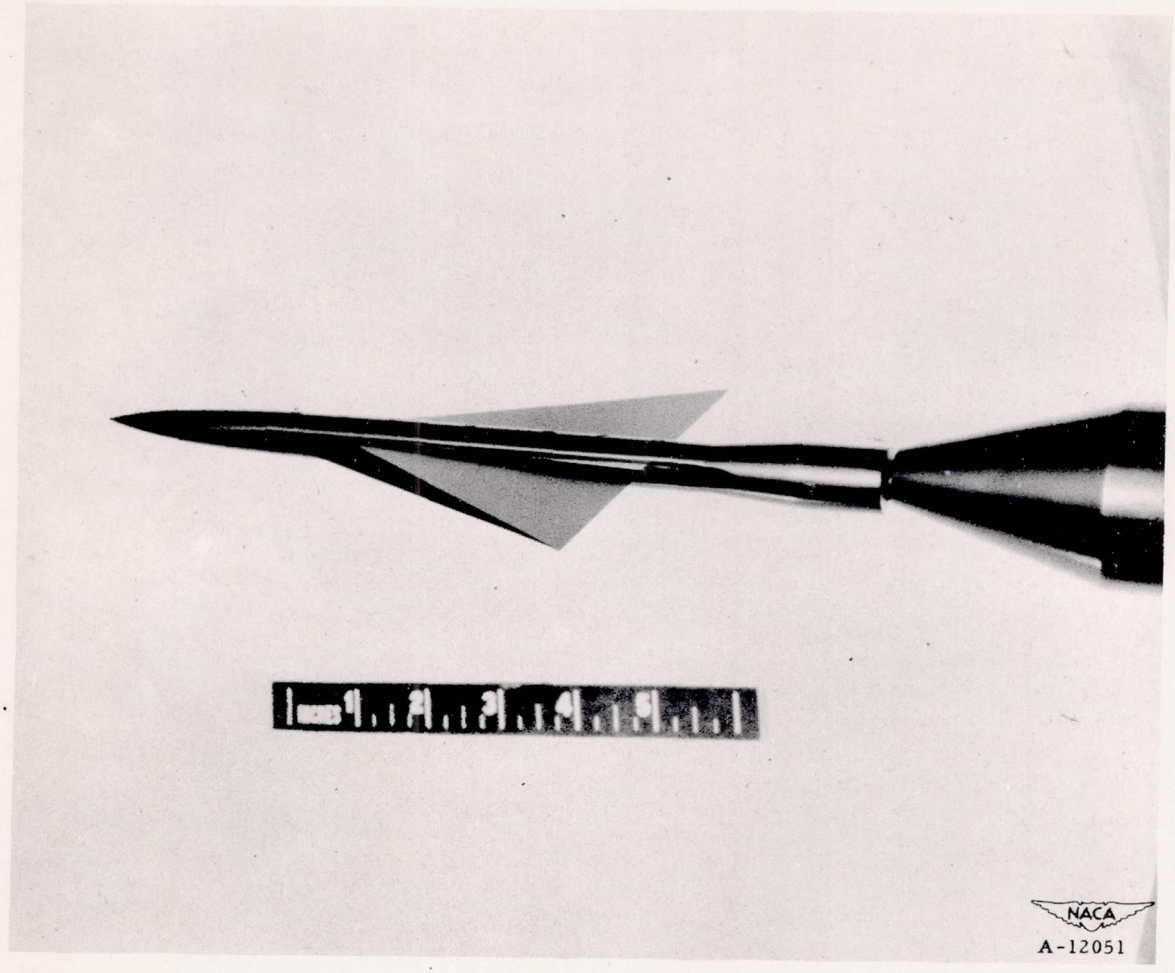


Figure 2.- Photograph of triangular wing and body.

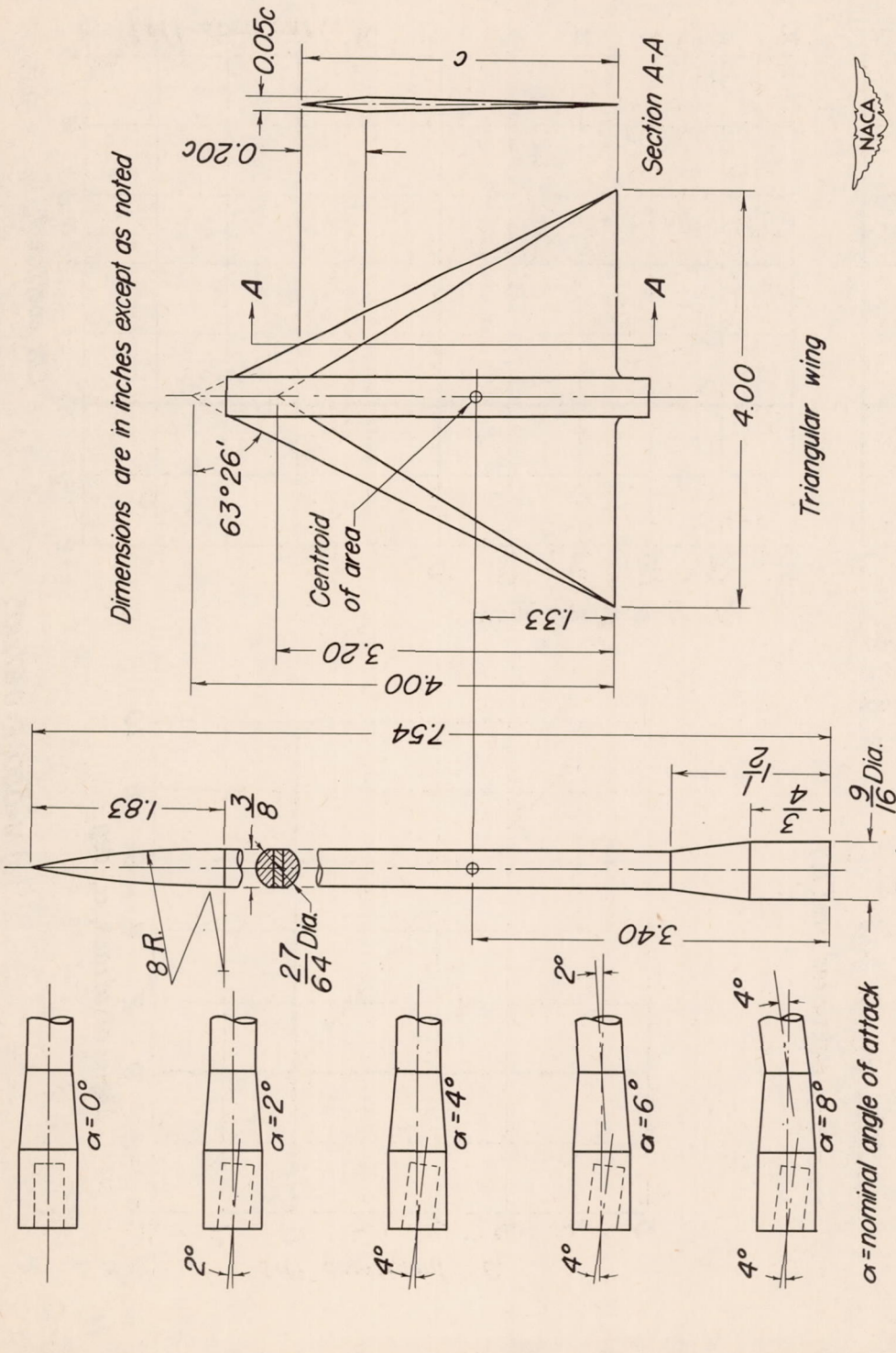


Figure 3.-Sketch of triangular wing and body.

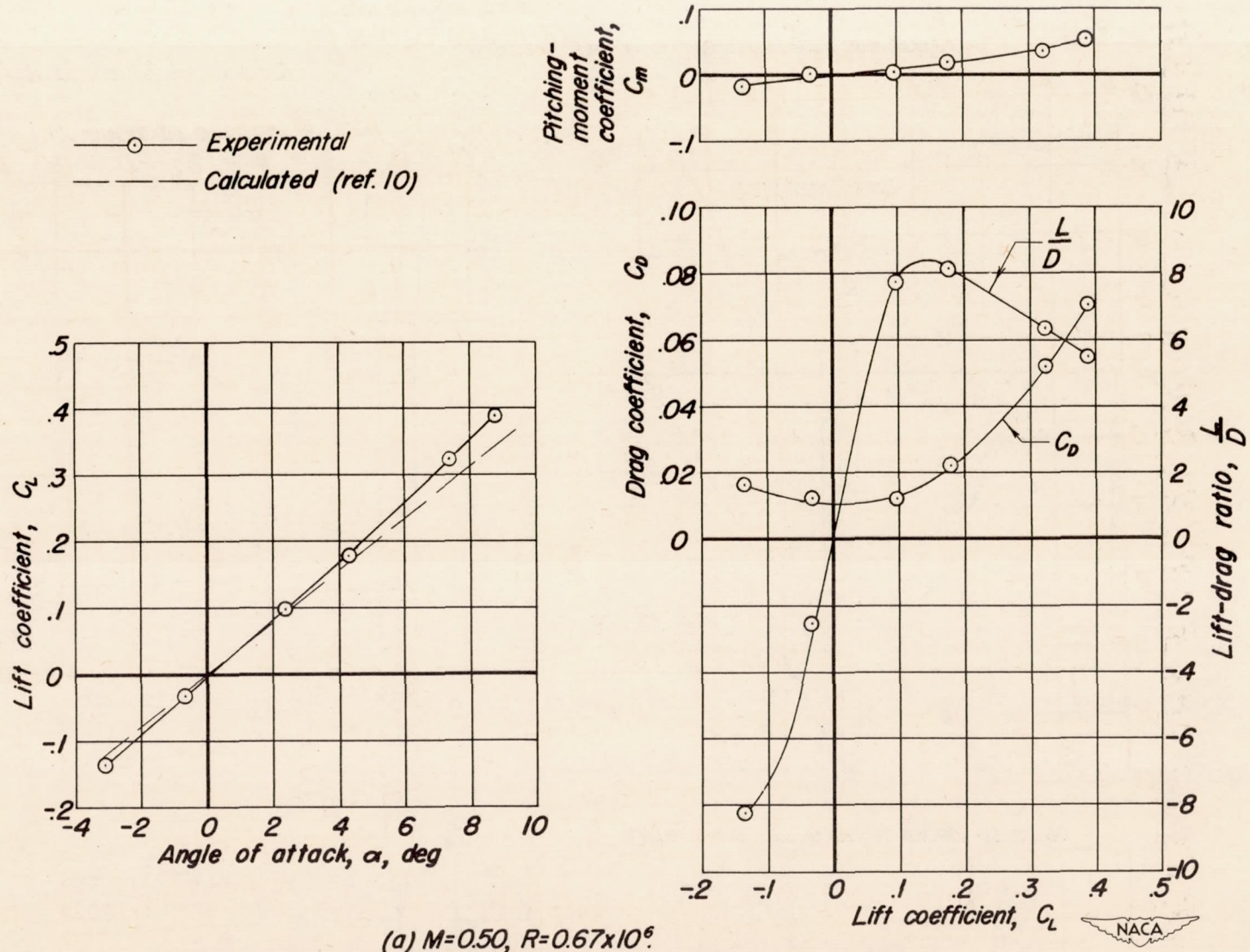


(a) M=0.50, R=0.67x10$^6$.

Figure 4.- Aerodynamic characteristics of triangular wing and body.

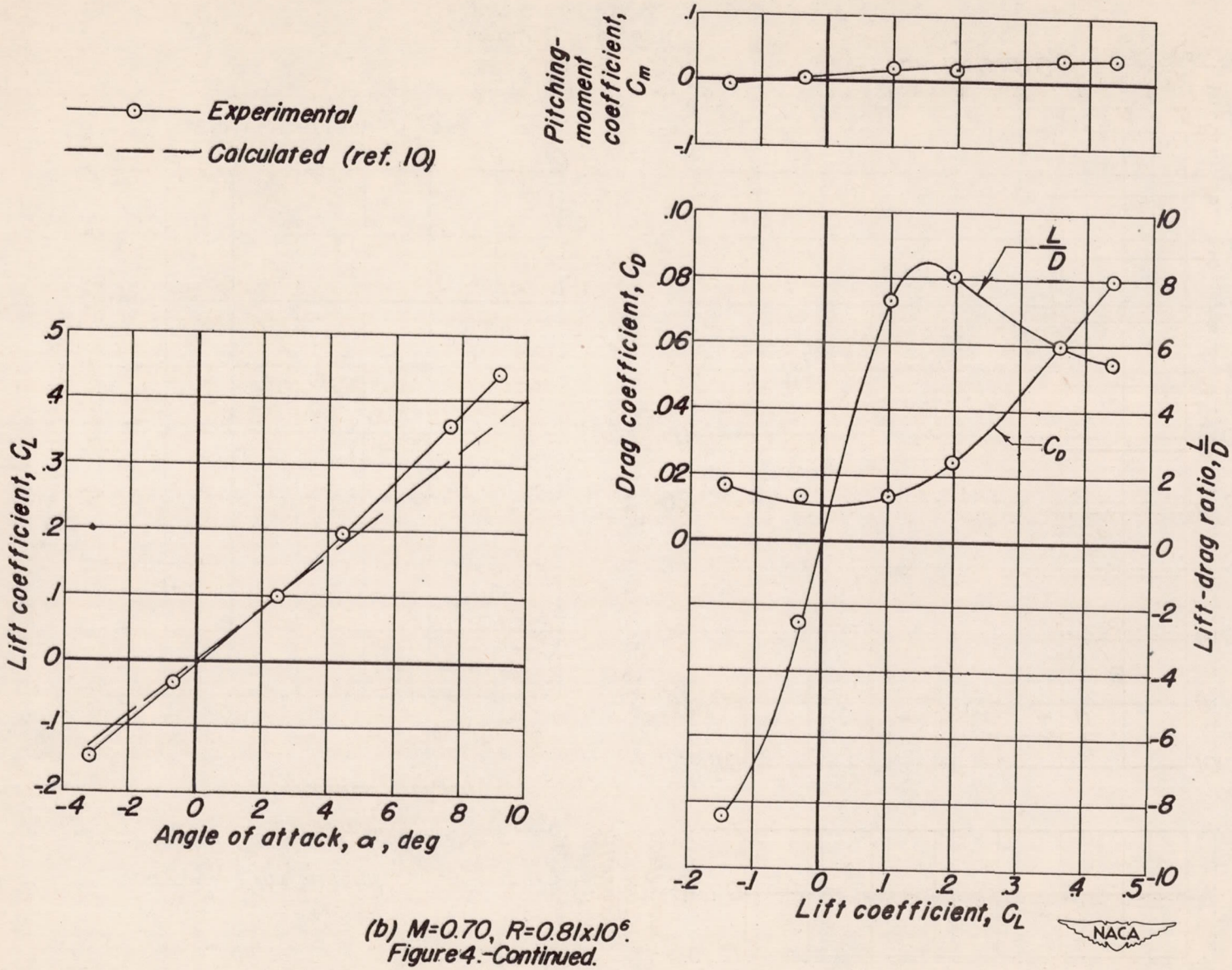


(b) M=0.70, R=0.81x10$^6$.
Figure 4.-Continued.

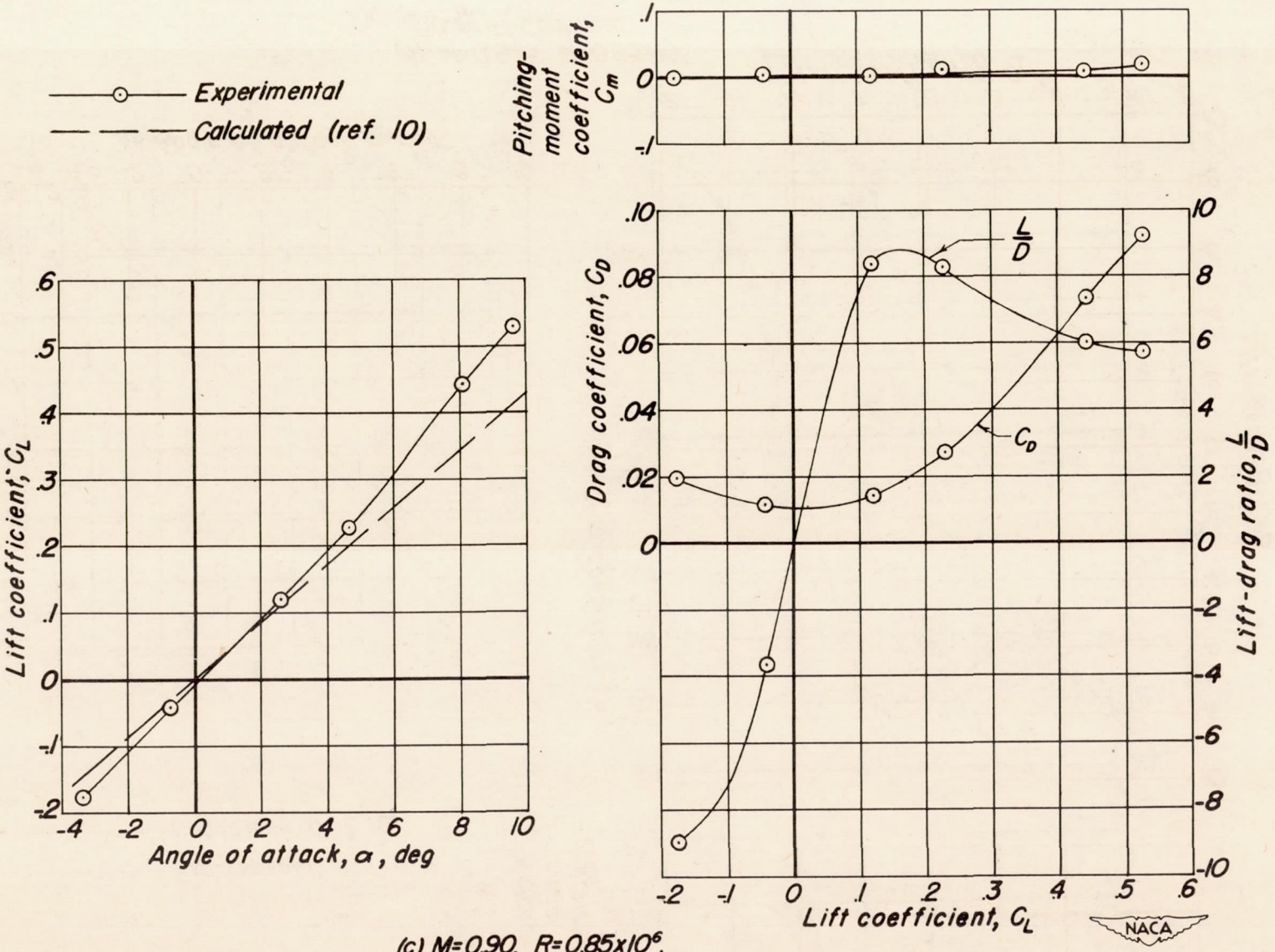


(c) M=0.90, R=0.85x10$^6$.
Figure 4.-Continued.

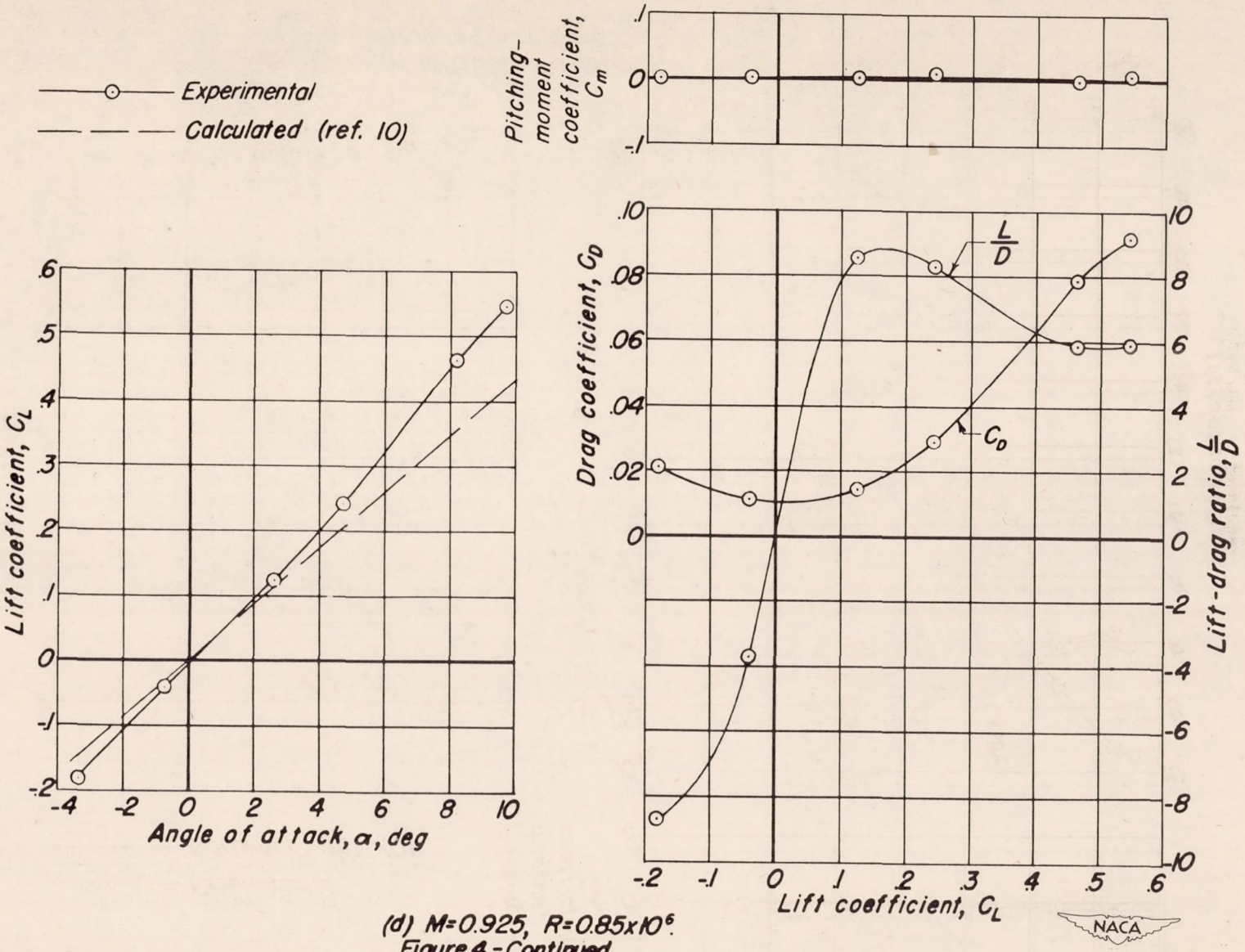


(d) M=0.925, R=0.85x10$^6$.
Figure 4.- Continued.

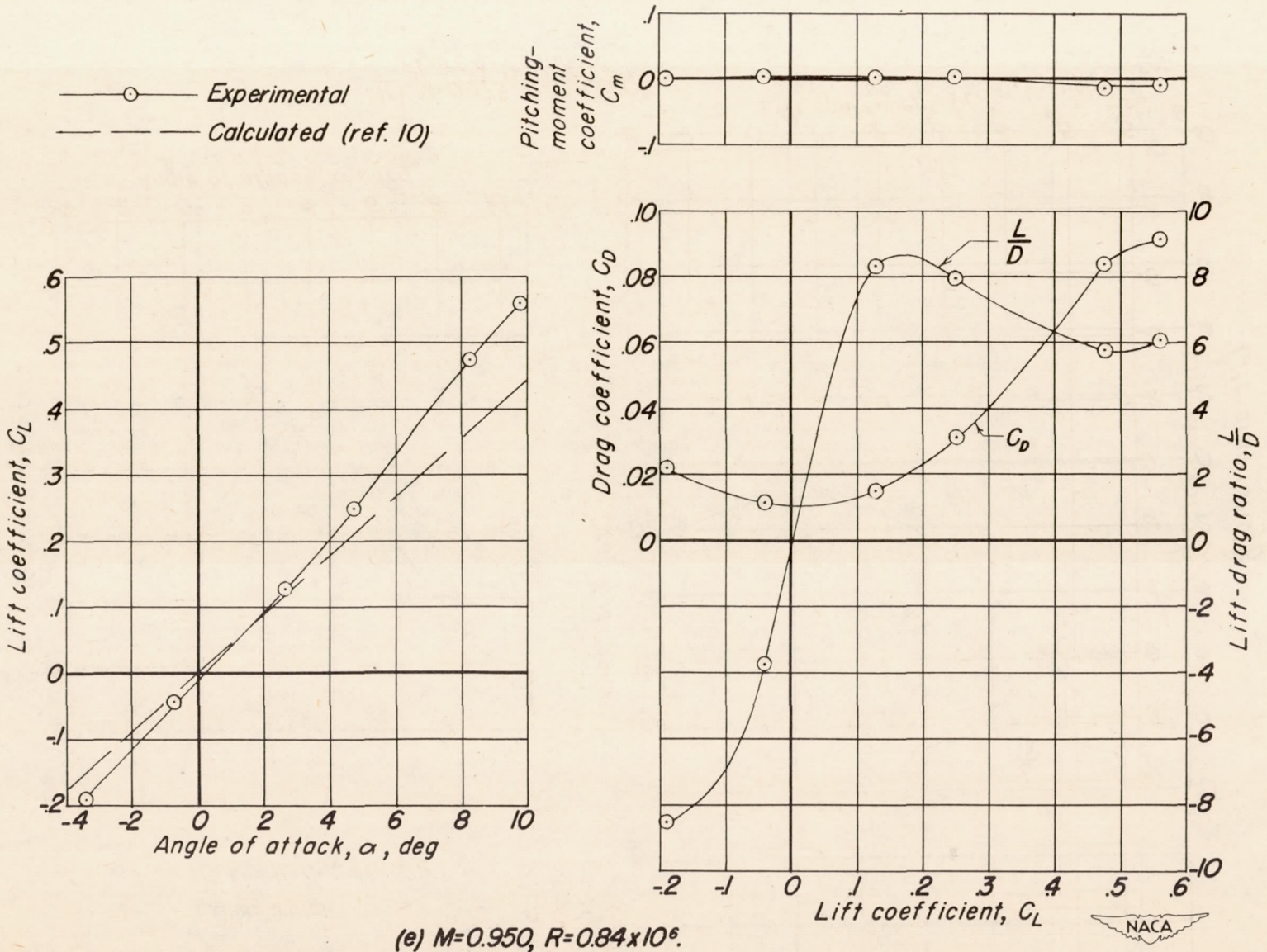


(e) M=0.950, R=0.84x10$^6$.

Figure 4.- Continued

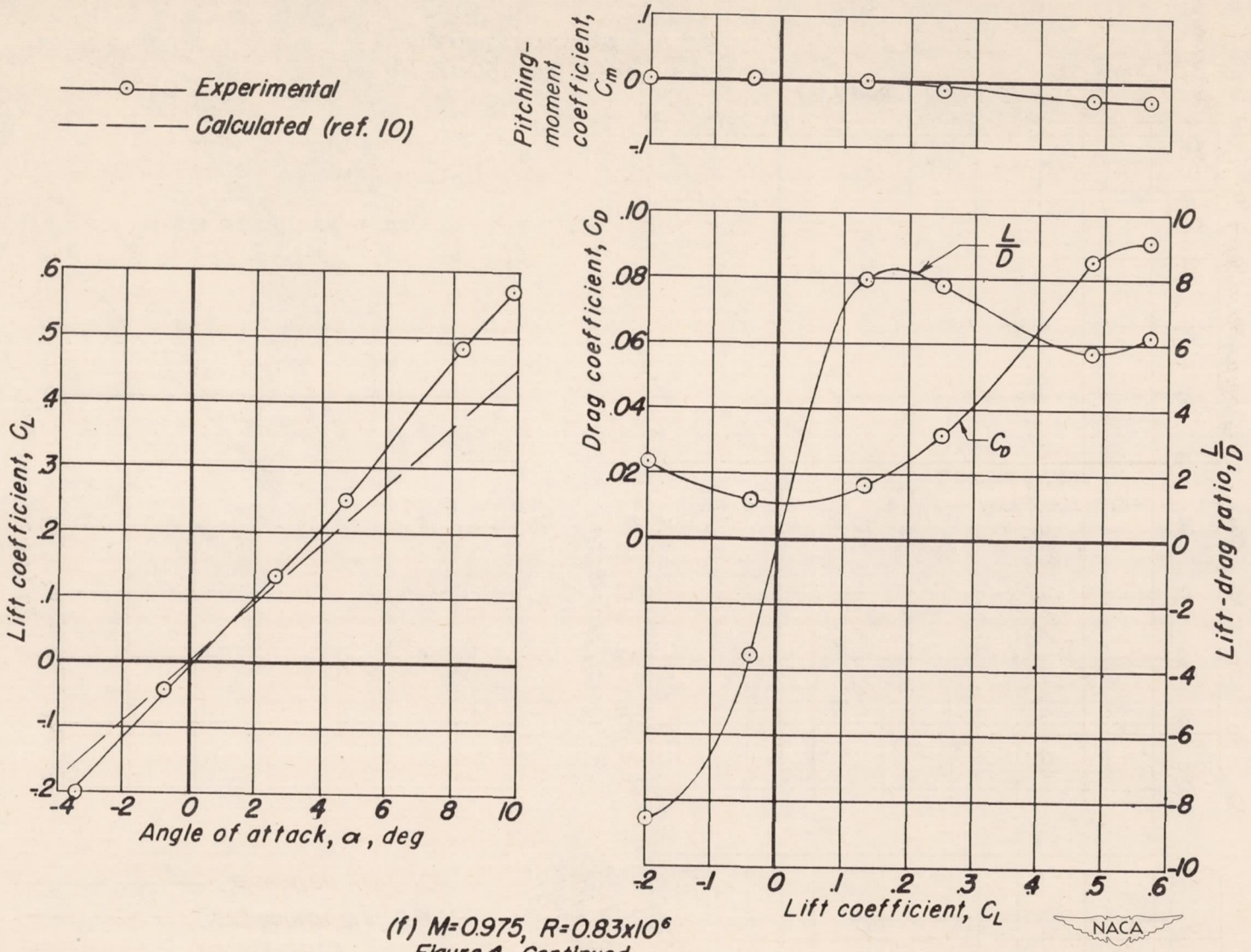


(f) M=0.975, R=0.83x10$^6$

Figure 4.- Continued.

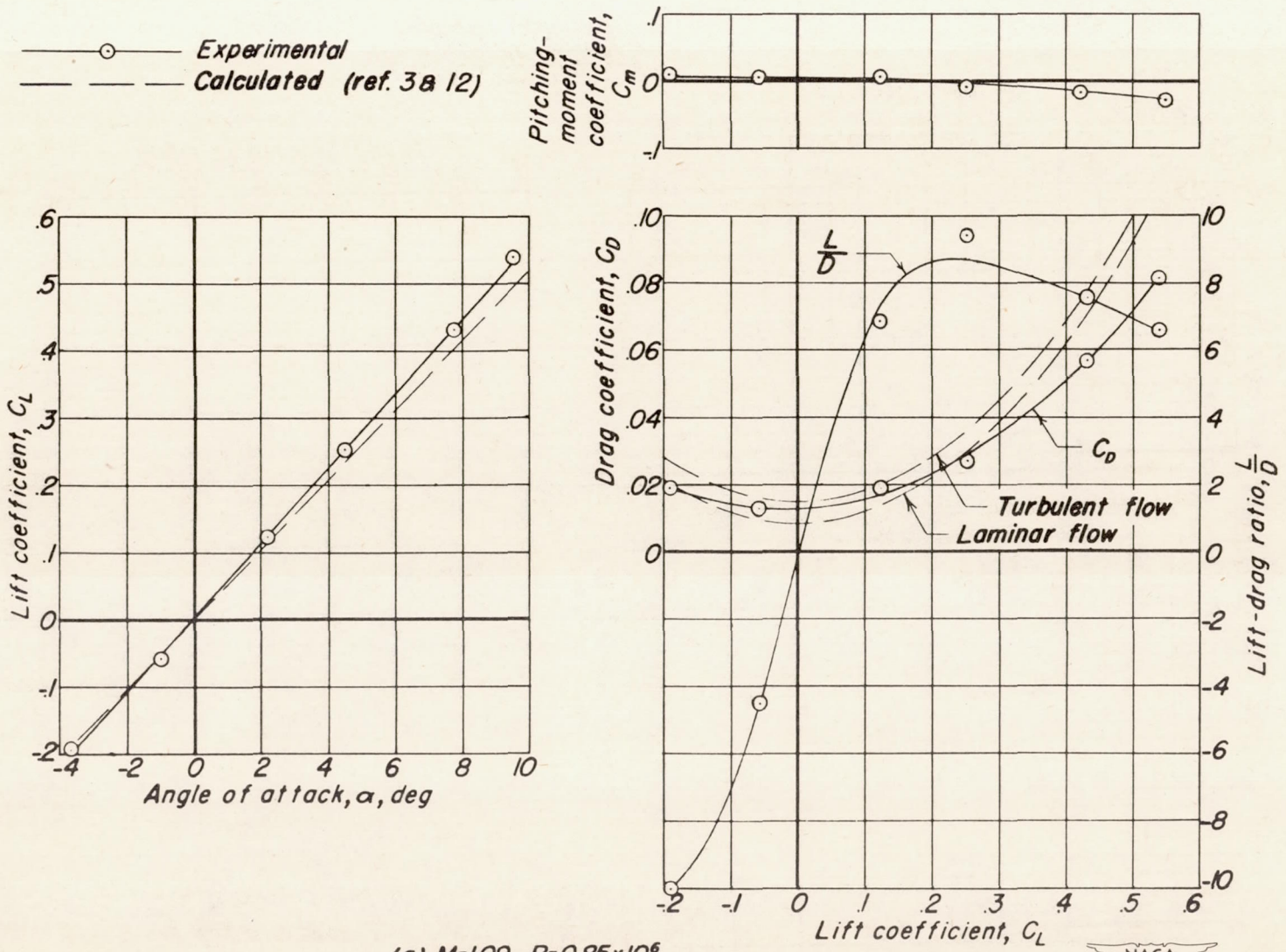


(g) M=1.09, R=0.85x10$^6$.
Figure 4.- Continued.

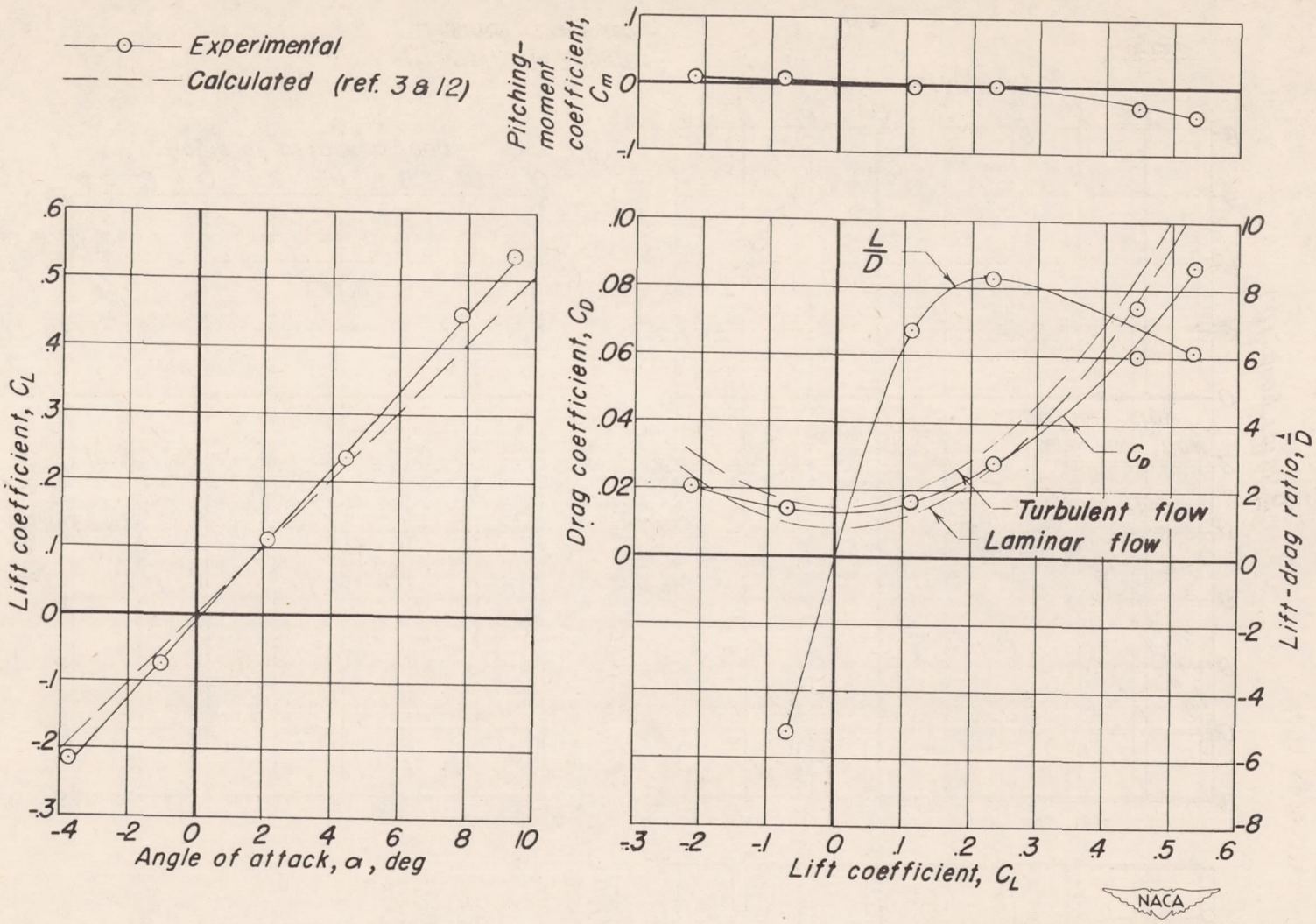


(h) M=1.12, R=0.85x10$^6$
Figure 4.- Continued.

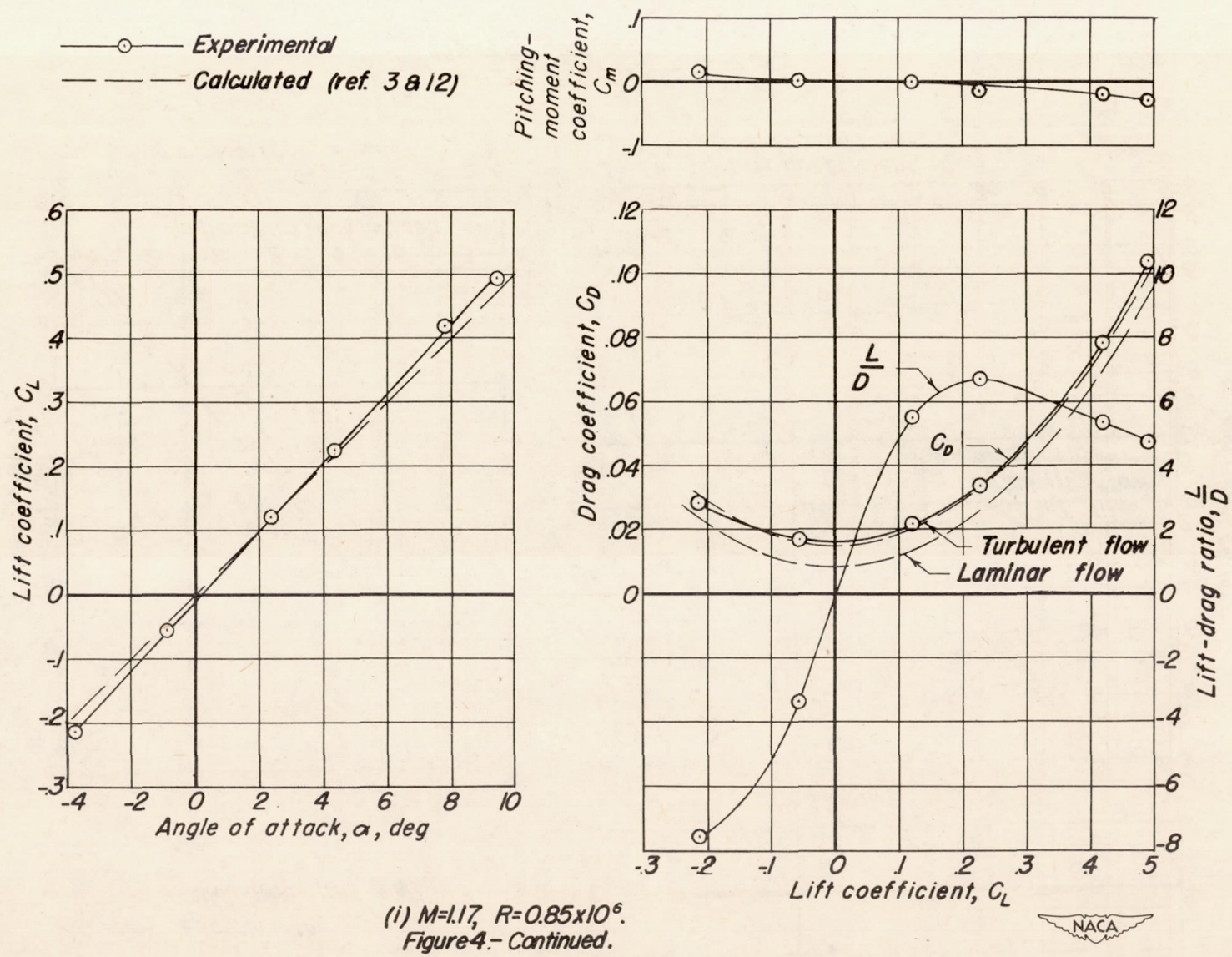


(i) M=1.17, R=0.85x10$^6$.

Figure 4.- Continued.

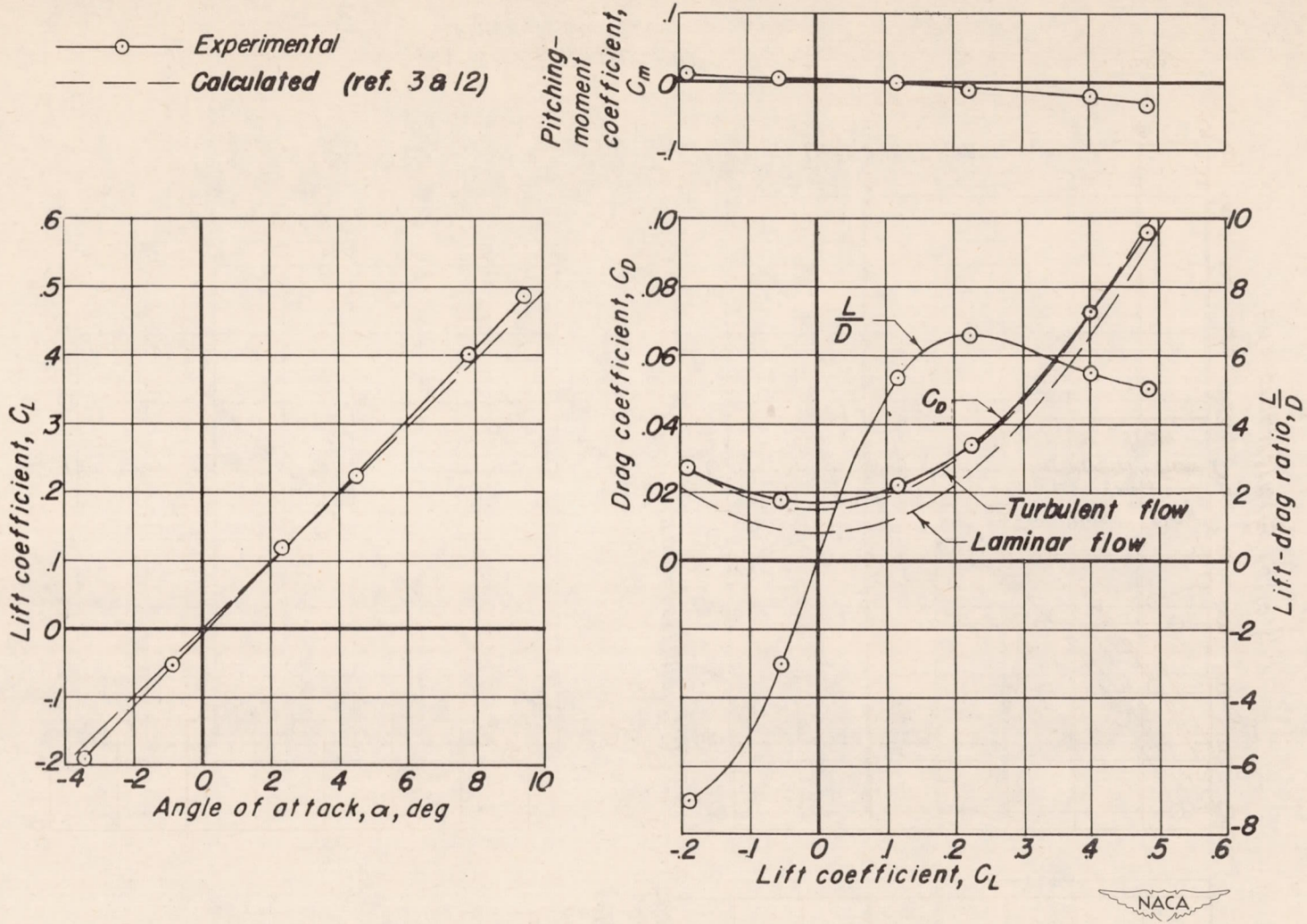


(j) M=1.20, R=0.85x10$^6$.
Figure 4.- Continued.

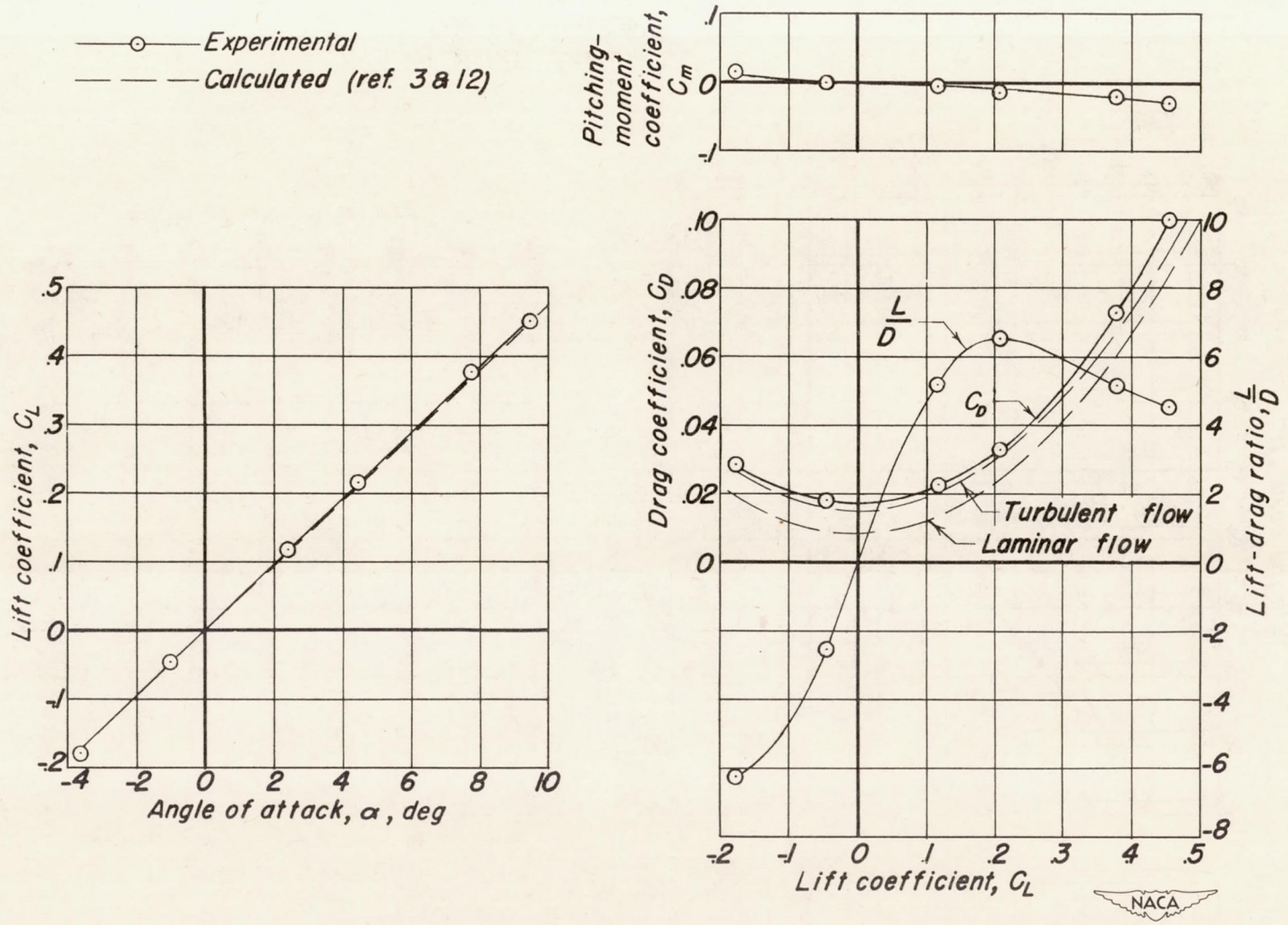


(k) M=1.29, R=0.85 x $10^6$.
Figure 4.-Continued.

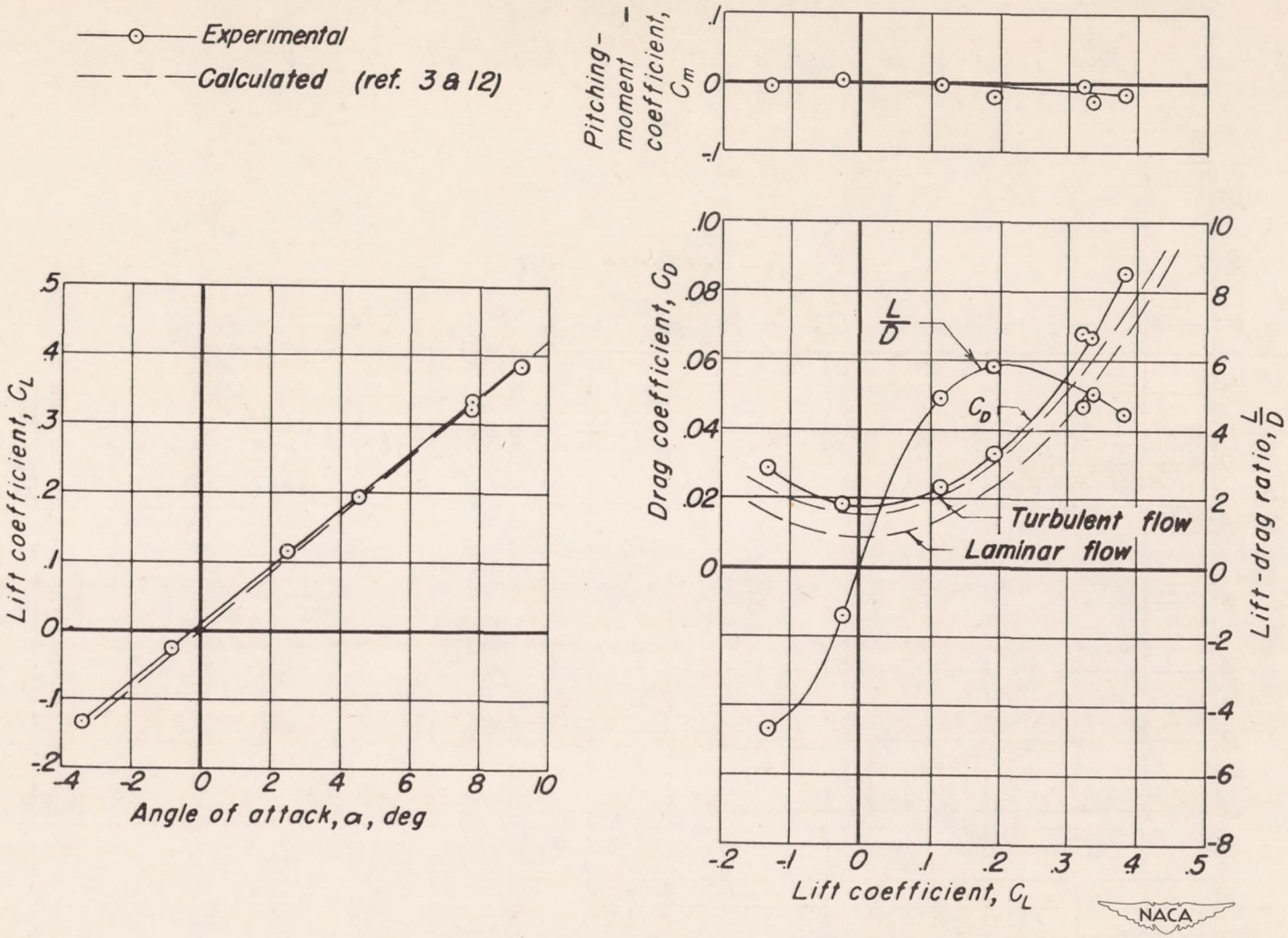


(l) M=1.49, R=0.83x10$^6$.

Figure 4.- Concluded.

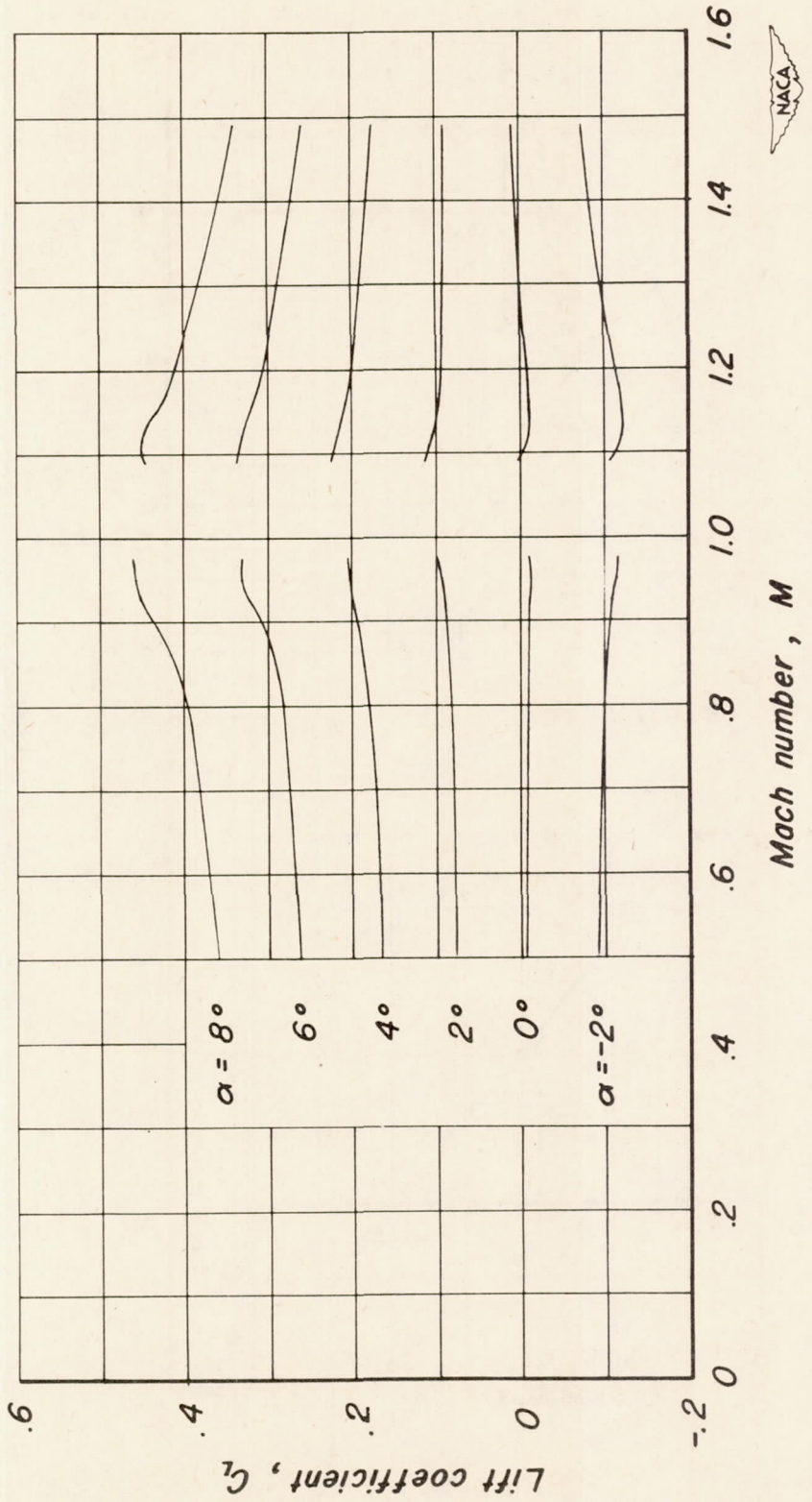


Figure 5.-Variation of lift coefficient with Mach number at constant angle of attack.

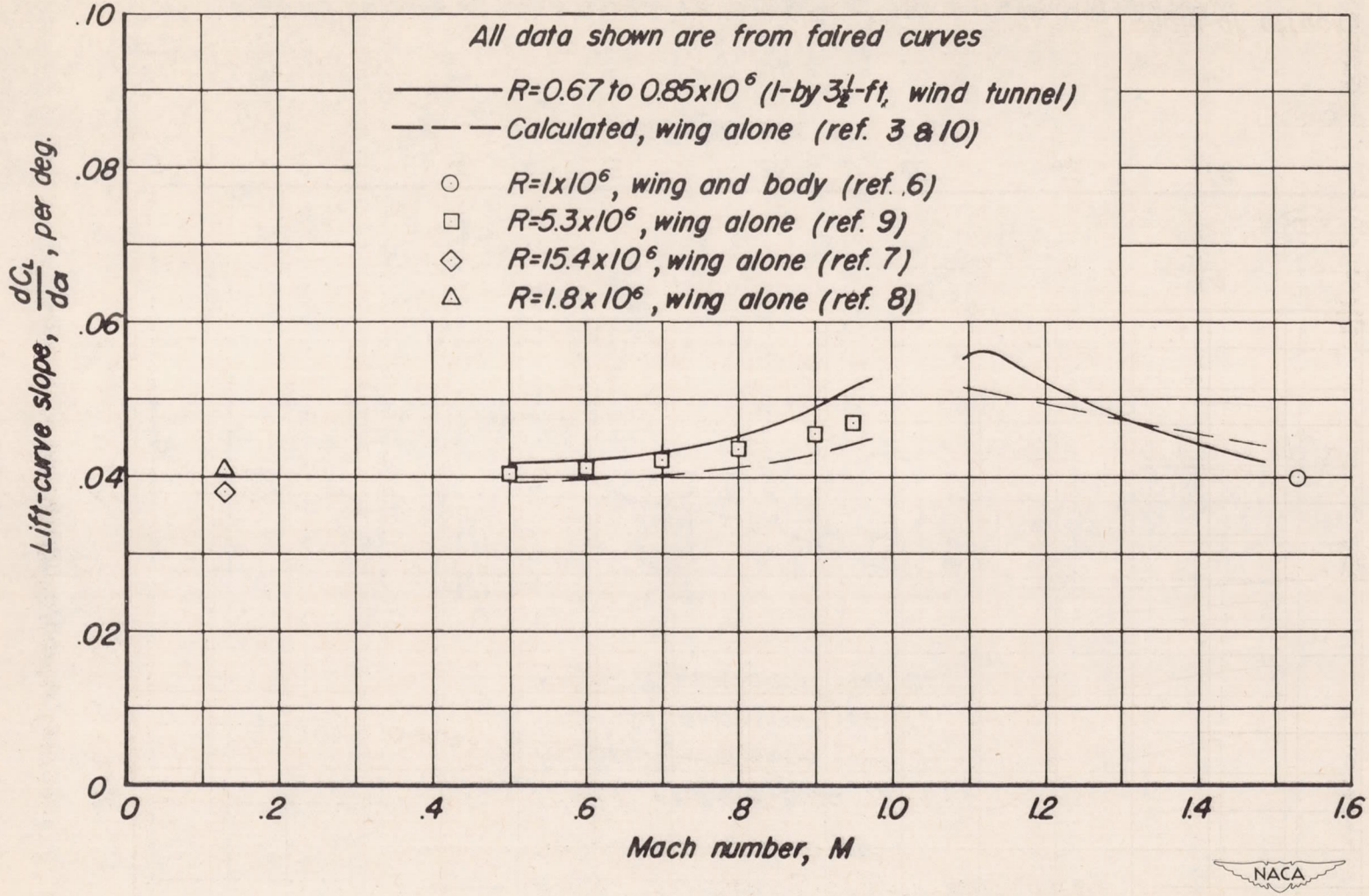


Figure 6.- Effect of Mach number on lift-curve slope.

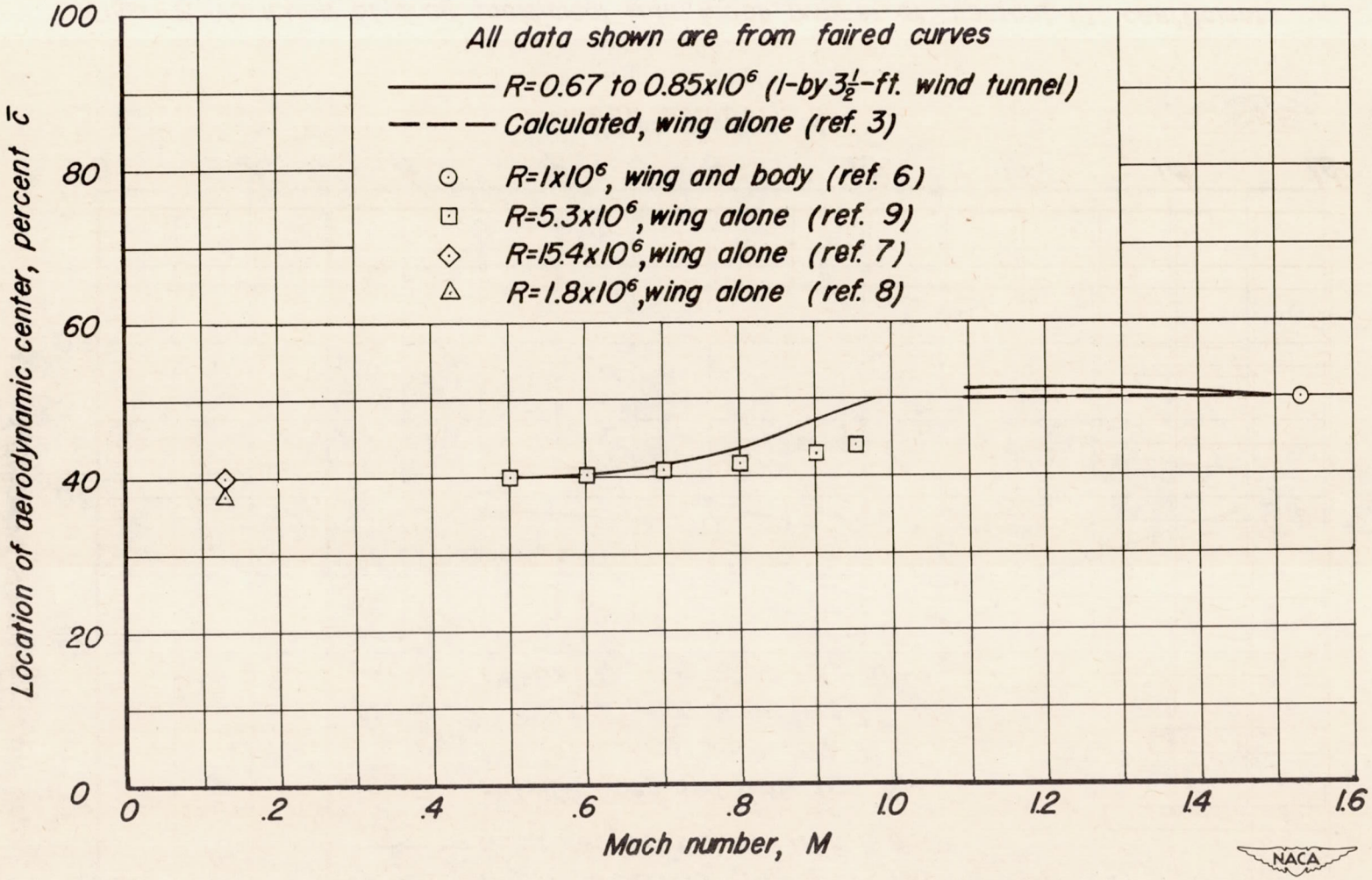


Figure 7.-Effect of Mach number on location of the aerodynamic center.

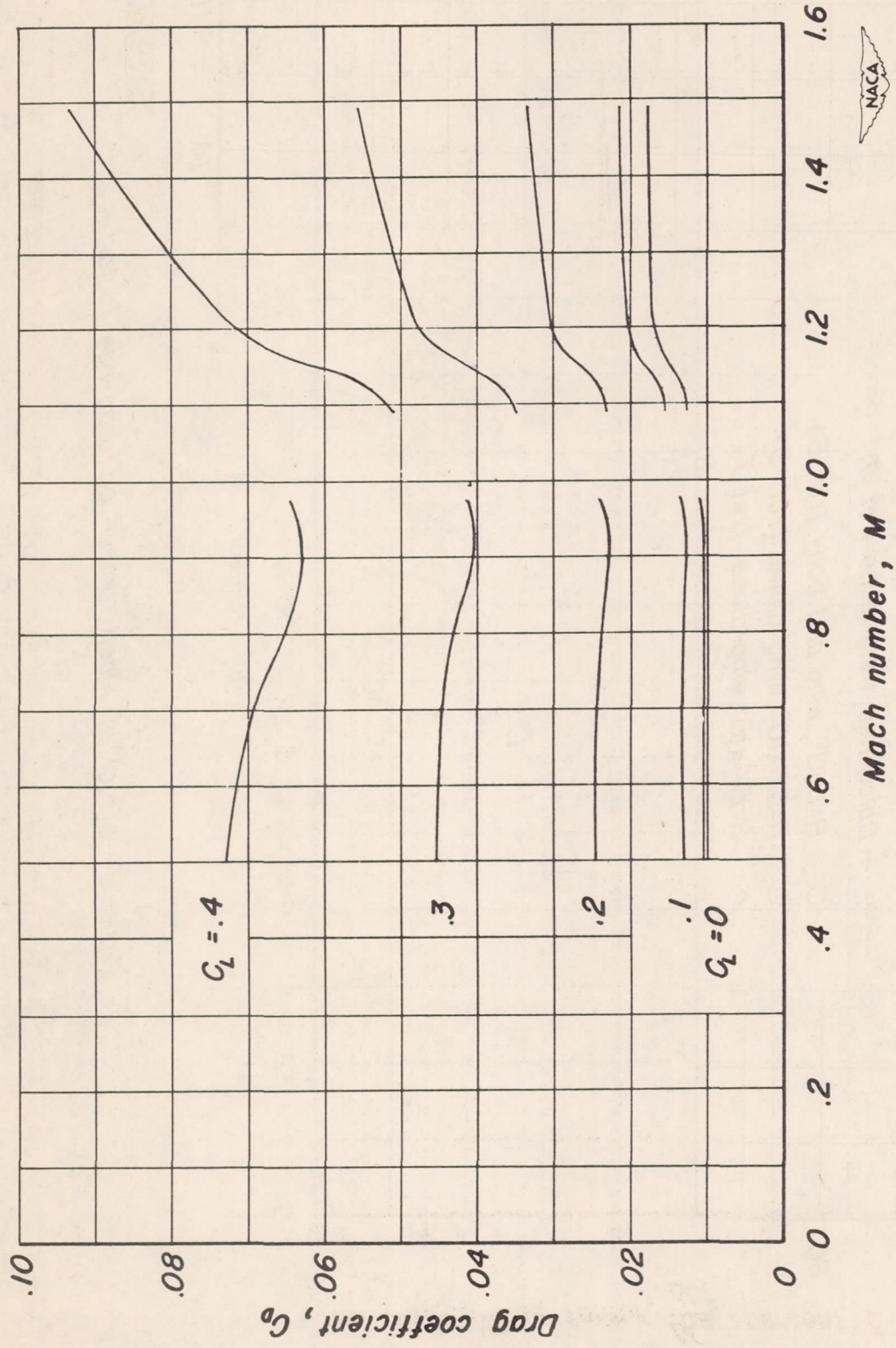


Figure 8.-Variation of drag coefficient with Mach number at constant lift coefficient.

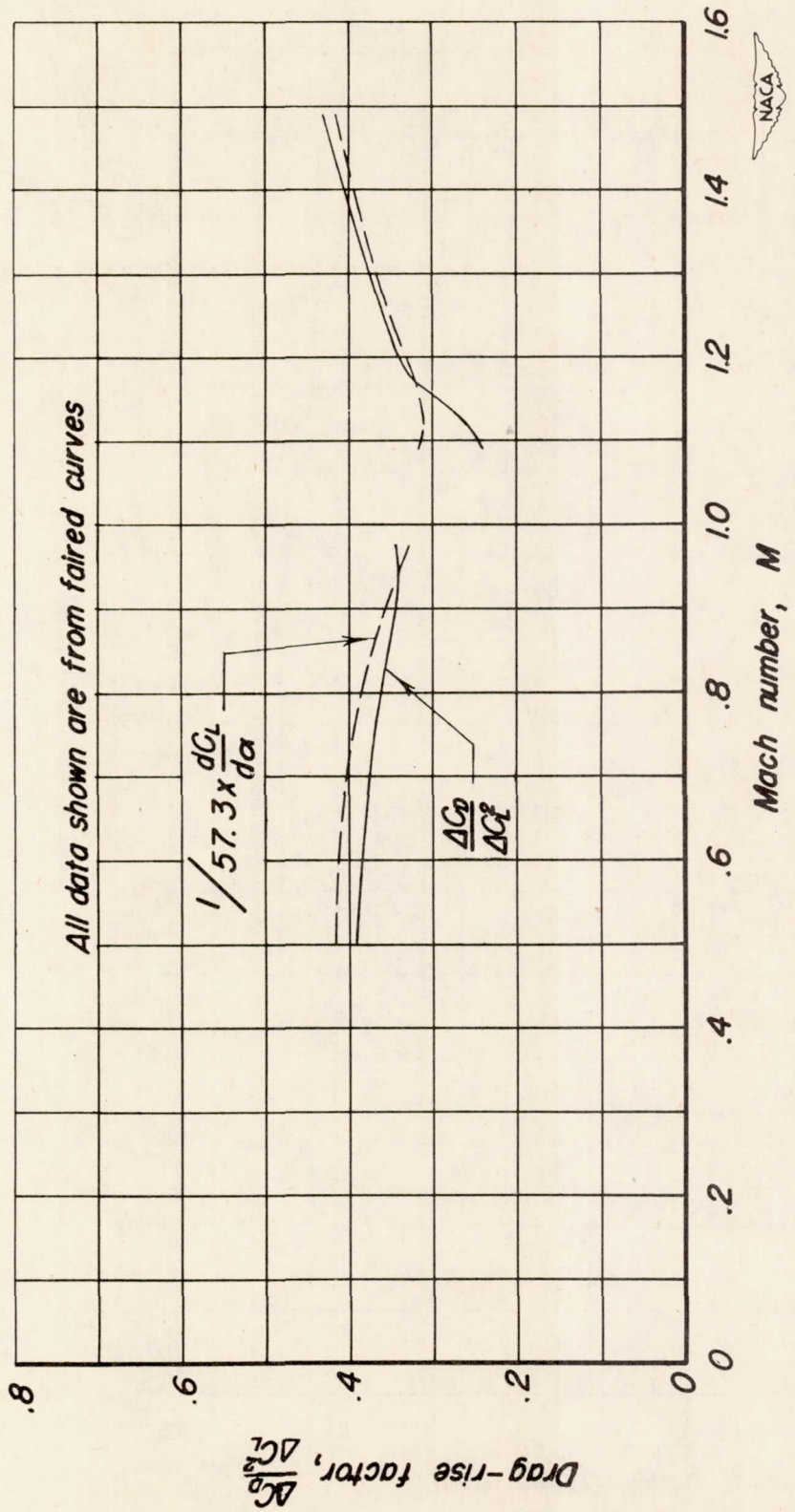


Figure 9.- Effect of Mach number on drag-rise factor.

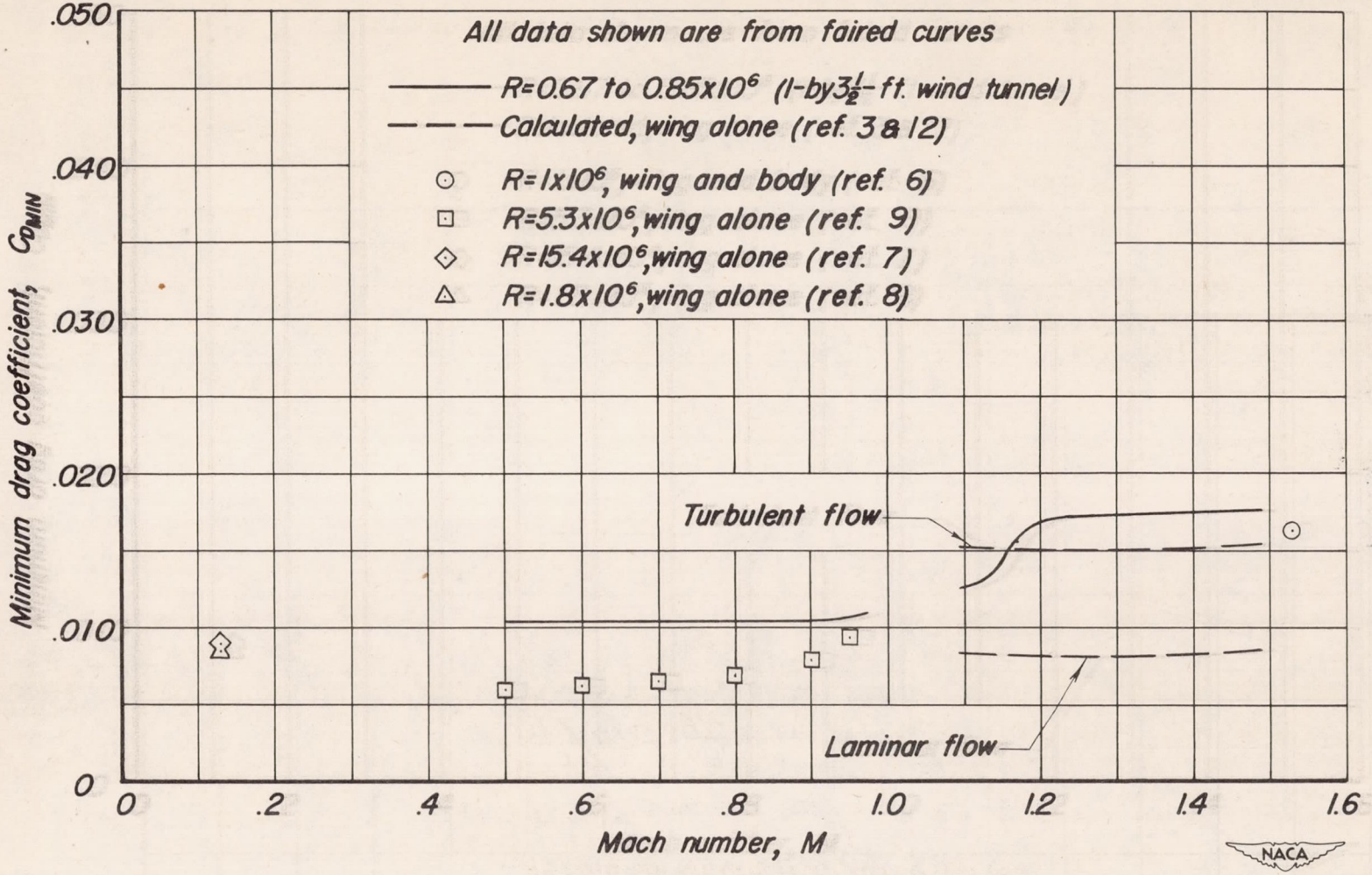


Figure 10.-Effect of Mach number on minimum drag coefficient.

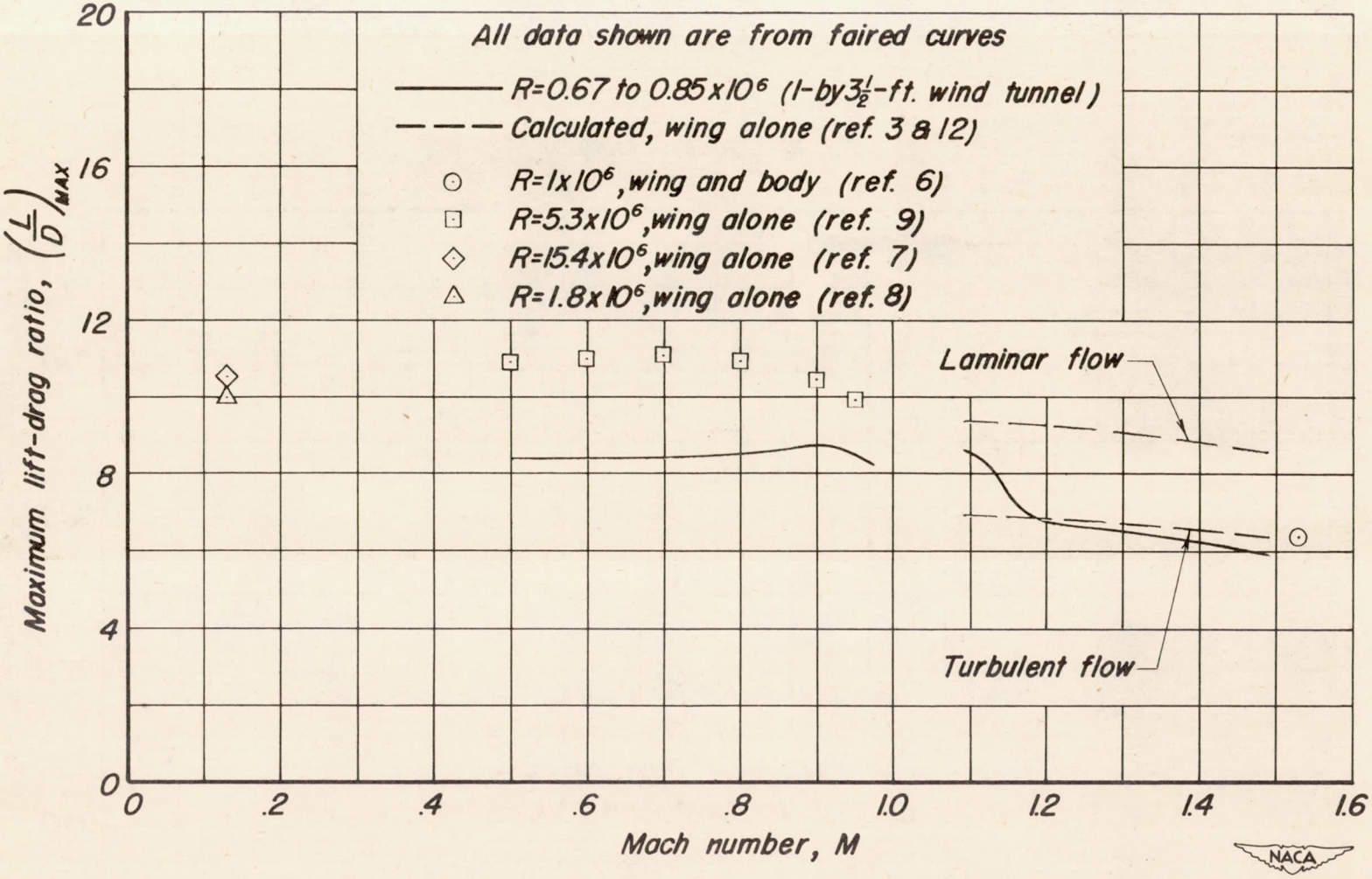


Figure 11.-Effect of Mach number on maximum lift-drag ratio.

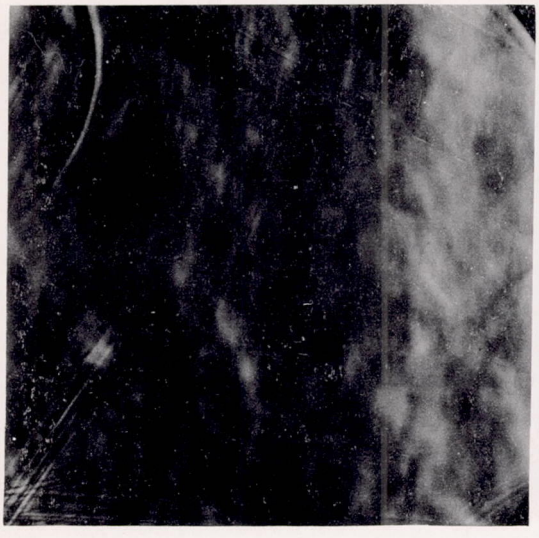

(a) Air stream off.

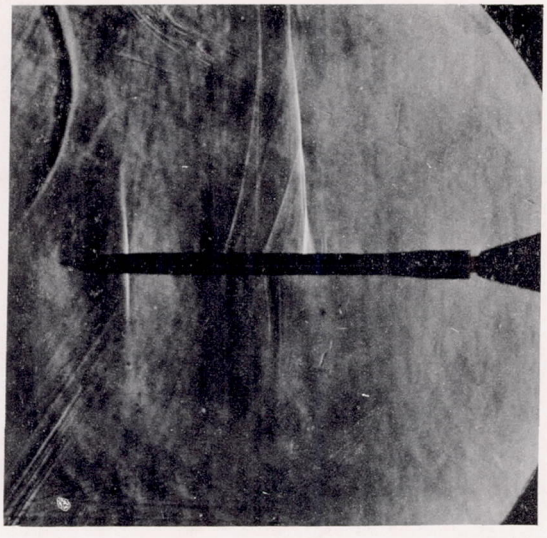

(b) M = 0.95, side view.

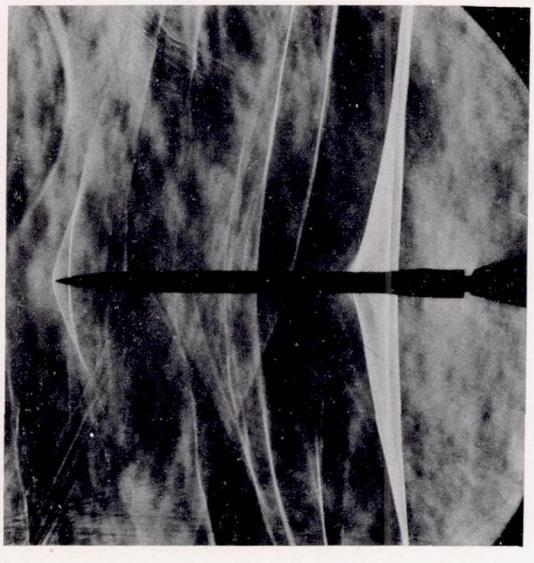

(c) M = 1.09, side view.

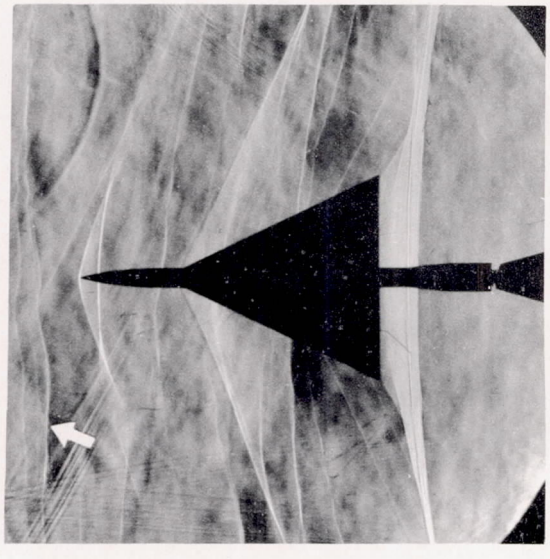

NACA
A-13017

(d) M = 1.09, plan view.

Figure 12.- Typical schlieren photographs of the side and plan views of the model at several Mach numbers.

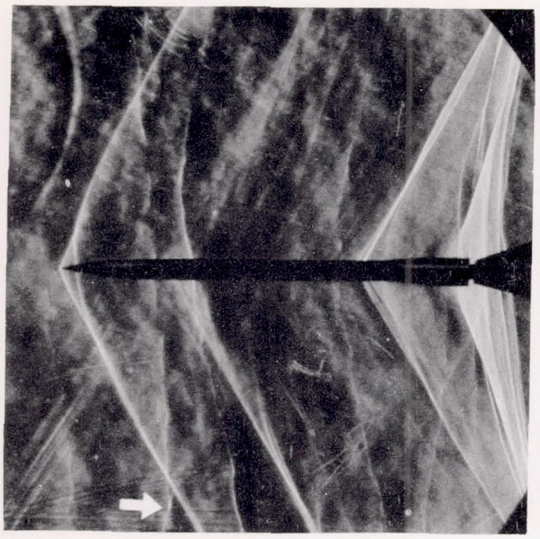

(e) M = 1.12, side view.

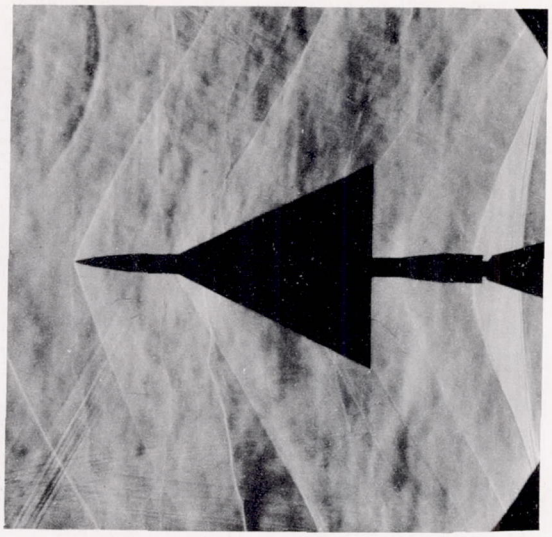

(f) M = 1.12, plan view.

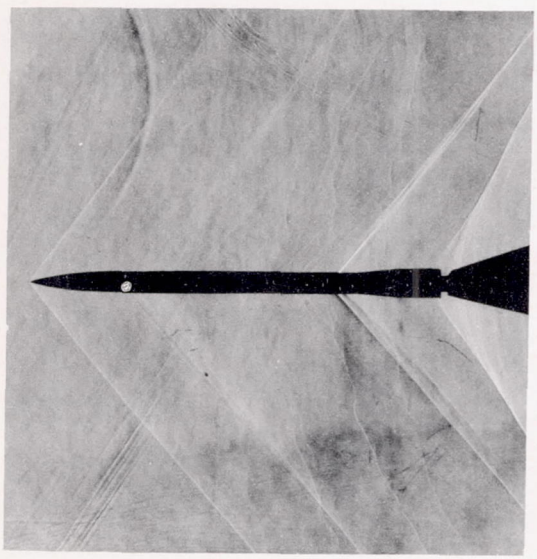

(g) M = 1.29, side view.

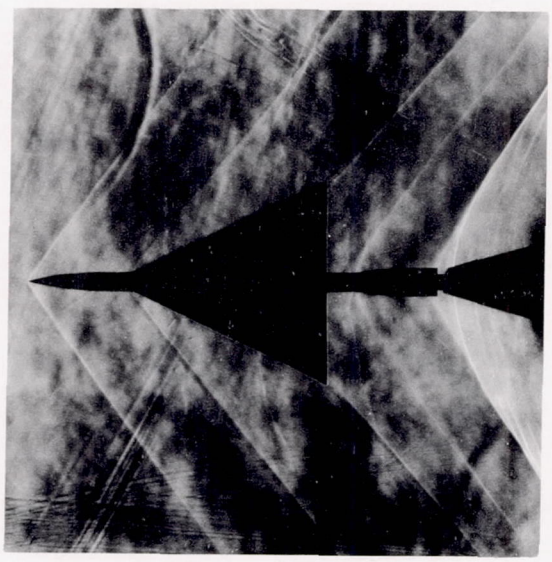

NACA
A-13018

(h) M = 1.29, plan view.

Figure 12.- Continued.

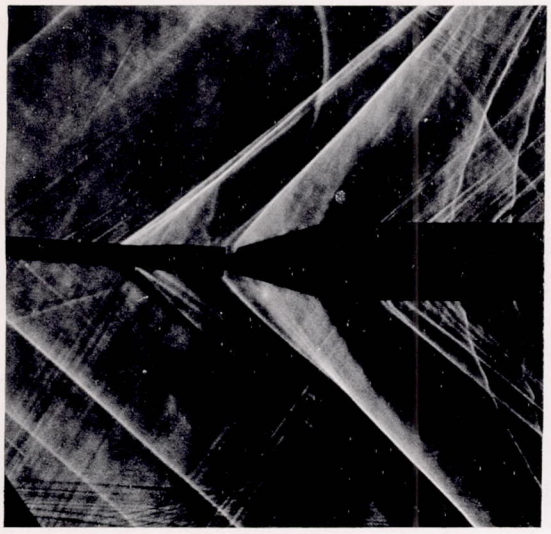

(i) M = 1.49, side view.

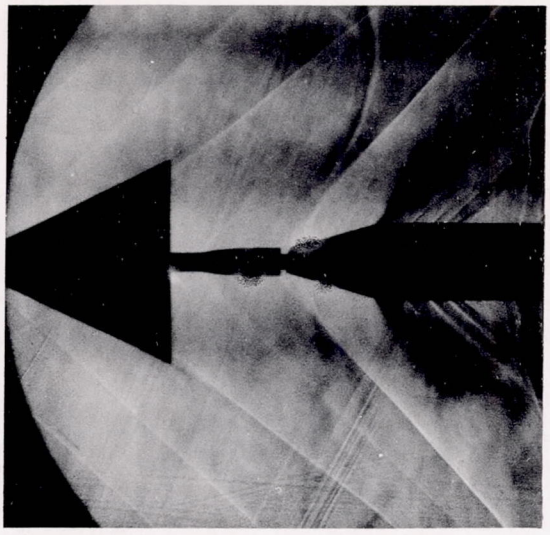

NACA
A-13019

(j) M = 1.49, plan view.

Figure 12.- Concluded.